



# Equilibrium and disequilibrium processes across the greenschist–amphibolite transition zone in metabasites

Paul G. Starr<sup>1,2</sup> · David R. M. Pattison<sup>1</sup>

Received: 18 October 2018 / Accepted: 5 February 2019 / Published online: 15 February 2019  
© Springer-Verlag GmbH Germany, part of Springer Nature 2019

## Abstract

Documentation of textures, modes and compositions of minerals in metamorphosed basalts across two greenschist-to-lower amphibolite facies sequences (Flin Flon, Manitoba and Rosslund, British Columbia) was combined with a compilation of the literature data to assess equilibrium and disequilibrium processes across this important transition zone. At Flin Flon and Rosslund, the greenschist–amphibolite facies transition occurs over a narrow spatial interval marked by hornblende-in, oligoclase-in and actinolite-out isograds. The data suggest the existence of stable miscibility gaps separating coexisting actinolite and hornblende, and coexisting albite and oligoclase, in the lowermost amphibolite facies. However, actinolite and hornblende show a divergence in compositions going upgrade across the oligoclase-in isograd, suggestive of disequilibrium between the new, progressively more aluminous hornblende and metastably persisting actinolite. Likewise, coexisting albite and oligoclase compositions show no evidence for converging compositions at higher temperatures, suggesting they do not remain in equilibrium across a miscibility gap. Compositional gaps within epidote phases are attributed to disequilibrium preservation of lower grade epidote compositions to higher grade conditions, rather than the existence of a miscibility gap at greenschist and amphibolite facies conditions. Recognition of equilibrium and disequilibrium relations highlights the difficulty of using natural compositional datasets to extract information on miscibility gaps and more generally to extract  $a$ – $X$  relationships. The greenschist-to-amphibolite facies transition is controlled principally by the consumption of chlorite, which primarily occurs upon crossing the oligoclase-in isograd, concomitant with conversion of actinolite to hornblende and albite to oligoclase. The result is a focused pulse of devolatilization over a small spatial and thermal interval.

**Keywords** Disequilibrium · Equilibrium · Greenschist facies · Amphibolite facies · Miscibility gaps · Metamorphic devolatilization

---

Communicated by Daniela Rubatto.

**Electronic supplementary material** The online version of this article (<https://doi.org/10.1007/s00410-019-1553-y>) contains supplementary material, which is available to authorized users.

---

✉ Paul G. Starr  
starrp@bc.edu

<sup>1</sup> Department of Geoscience, University of Calgary, 2500 University Drive NW, Calgary, AB T2N 1N4, Canada

<sup>2</sup> Present Address: Department of Earth and Environmental Sciences, Boston College, 140 Commonwealth Avenue, Chestnut Hill, MA 02467, USA

## Introduction

Our current knowledge of metabasites, both in terms of our understanding of the evolution of natural mineral assemblages with grade, and our ability to generate realistic phase equilibria, is currently behind knowledge of their metapelitic counterparts. Whereas metapelites develop low-variance mineral assemblages involving the appearance and disappearance of characteristic index minerals (e.g., garnet, staurolite, kyanite), meta-basalts, especially in the greenschist and amphibolite facies, show relatively small changes in mineral assemblage with grade and are instead dominated by changes in mineral composition and modal proportions (e.g., Cooper 1972; Maruyama et al. 1983; Elmer et al. 2006).

An exception to this situation occurs in the transition from greenschist facies to amphibolite facies. This important transition is marked by a complex set of reactions

involving the breakdown of combinations of actinolite, epidote, albite, and chlorite, in favour of hornblende and calcic plagioclase (e.g., Cooper 1972; Maruyama et al. 1983; Begin 1992), and is associated with significant devolatilization that has been linked to formation of economically valuable ore deposits (e.g., orogenic gold deposits) (e.g., Powell et al. 1991; Elmer et al. 2006; Phillips and Powell 2010). Metabasites in the greenschist–amphibolite transition zone are characterised by the coexistence of multiple amphibole, plagioclase, and epidote group minerals (e.g., Cooper 1972; Maruyama et al. 1982; Begin and Carmichael 1992; Grapes and Hoskin 2004). Understanding the relationship between these minerals, and whether they reflect equilibrium or disequilibrium coexistence, is crucial for accurately interpreting pressure–temperature ( $P$ – $T$ ) conditions from these rocks and for understanding the important metamorphic processes, such as devolatilization reactions, that occur across the transition zone.

Considerable research has focused on compositional gaps within the key mineral groups across the transition zone, especially amphibole, plagioclase, and epidote group minerals (e.g., Cooper and Lovering 1970; Cooper 1972; Graham 1974; Hietanen 1974; Grapes and Graham 1978; Carpenter 1981; Maruyama et al. 1982, 1983; Robinson 1982; Grapes and Otsuki 1983; Begin and Carmichael 1992; Terabayashi 1993). The nature of the coexistence of some of these minerals within the greenschist–amphibolite transition zone, particularly the coexisting amphiboles, actinolite and hornblende, continues to fuel debate. From an equilibrium perspective, the existence of miscibility gaps has been advanced to account for the coexistence of more than one member of individual mineral groups (e.g., Klein 1969; Cooper and Lovering 1970; Smelik et al. 1991; Begin and Carmichael 1992; Zingg 1996). However, disequilibrium and preservation of lower grade phases as metastable relics can also produce coexistence of multiple phases (e.g., Graham 1974; Grapes 1975; Sampson and Fawcett 1977; Grapes and Graham 1978).

In this study, the textures, modes and compositions of minerals in metamorphosed basalts across two prograde greenschist-to-lower amphibolite facies sequences (Flin Flon, Manitoba and Rossland, British Columbia) are combined with data from the literature to better understand the controlling processes that occur in this important metamorphic interval. These observations are used to assess: (1) the possible existence and shape of miscibility gaps within the key mineral groups; (2) evidence for disequilibrium; (3) implications for the metamorphic devolatilization occurring across the transition zone; and (4) the reliability of using natural datasets to derive miscibility compositional limits.

## Geological background

### Flin Flon–Glennie complex, Manitoba/Saskatchewan

The Flin Flon–Glennie complex (FFGC) comprises part of the internal zone of the Trans-Hudson Orogen (THO) in Saskatchewan and Manitoba (Fig. 1a, b), separating the Archean Superior, Hearne and Sask cratons that were amalgamated during Trans-Hudson orogenesis (e.g., Lucas et al. 1996; Ansdell 2005). The accreted tectono-stratigraphic terranes that comprise the FFGC consist predominantly of juvenile arc material, in addition to ocean floor rocks, oceanic plateaus, ocean island basalts and plutonic arc rocks that range in age from 1.91 to 1.84 Ga (e.g., Stauffer 1984; Stern et al. 1995; Lucas et al. 1996).

The area in the vicinity of Flin Flon has attracted a considerable amount of research due to the presence of a number of large volcanogenic massive sulphide (VMS) deposits (Fig. 1b) (e.g., Syme and Bailes 1993; Digel and Gordon 1995; Stern et al. 1995; Lucas et al. 1996; Gale et al. 1999; DeWolfe and Gibson 2006; DeWolfe et al. 2009; Ames et al. 2016; Lafrance et al. 2016). The structure, plutonism, and stratigraphy within the Flin Flon domain reflect a complex regional tectonic history, which includes initial accretionary, collisional and post-collisional stages of the Trans-Hudson Orogeny (e.g., Lafrance et al. 2016). The Hidden and Louis Formations, which are the main units sampled for this study are dominated by pillowed basalt/basaltic andesite, mafic volcanoclastics, and hypabyssal dykes and sills (DeWolfe and Gibson 2006; DeWolfe et al. 2009). Unconformably overlying the Hidden and Louis Formations is the Missi group, a sedimentary package comprising conglomerate, sandstone and siltstone (Fig. 1b). The metamorphic grade in the Flin Flon area ranges from prehnite–pumpellyite facies to amphibolite facies, with metamorphic grade broadly increasing in a northerly direction (Fig. 1b) (Digel and Gordon 1995; this study).

### Rossland Group, British Columbia

The Rossland Group, located in southeastern British Columbia, forms part of the internal zone of the Canadian portion of the North American Cordillera (the Omineca Crystalline Belt) (e.g., Beddoe-Stephens 1982; Höy and Dunne 2001). The Omineca Crystalline Belt consists of metamorphosed and deformed rocks that separate the ancestral North American margin to the East from the terranes that were accreted as part of the Cordilleran Orogeny (e.g., Höy and Dunne 2001). The Rossland Group comprises a succession of early-to-mid-Jurassic clastic and

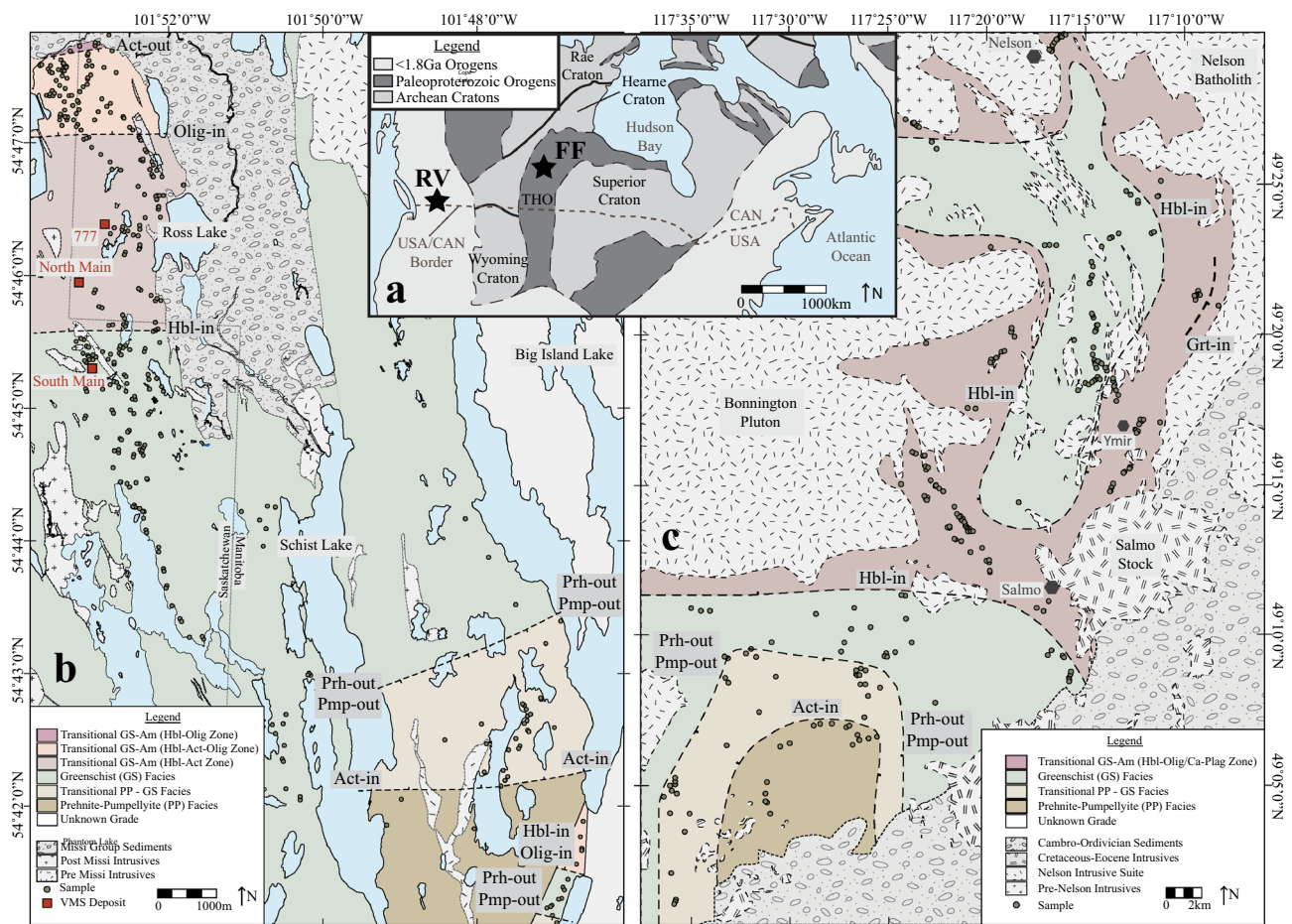


**Fig. 1** **a** Simplified large-scale geology map of North America showing the positioning of the major cratonic and orogenic belts. *THO* Trans-Hudson Orogen, *FF* Flin Flon field area, *RV* Rossland field area. Modified after Lucas et al. (1996); originally modified from Hoffman (1988). **b** Regional metamorphic isograd map for the Flin

Flon field area, superimposed on a simplified geology map. Sample sites with full mineral assemblage shown by brown dots. Volcanogenic massive sulphide (VMS) deposits shown by red squares. **c** Regional metamorphic isograd map for the Rossland field area, superimposed on a simplified geology map

volcanic rocks that are interpreted to be the youngest and most easterly of the volcanic arc units that comprise an arc terrane known as Quesnellia (e.g., Höy and Dunne 2001). Quesnellia was thrust onto the ancestral North American margin in the early Jurassic in the early stages of Cordilleran orogenesis. A number of plutonic bodies have been emplaced within the Rossland Group in the study area, ranging in age from early Jurassic to Eocene (Fig. 1c) (Sevigny and Parrish 1993; Höy and Dunne 2001). The most prominent intrusion is the Middle Jurassic Nelson Batholith (159–173 Ma; Sevigny and Parrish 1993; Ghosh 1995), which has a surface outcrop pattern consisting of a large ‘main body’ extending 50 km north of Nelson and an elongate ‘tail’ extending south close to the town of Ymir.

Previous studies of the metamorphism of the area have examined basaltic (Beddoe-Stephens 1981; Powell and Ghent 1996) and pelitic lithologies (Pattison and Vogl 2005; Tomkins and Pattison 2007; Pattison and Tinkham

2009), the latter restricted to the contact aureoles of the intrusions. Beddoe-Stephens (1981) suggested a gradual northward increase in metamorphic grade across the region, whilst Powell and Ghent (1996) later proposed a series of isograds suggesting a more irregular metamorphic gradient. Their isograds, showing a south-to-north transition from sub-greenschist-to-lower amphibolite facies over a distance of approximately 1.5 km moving towards the Bonnington and Nelson intrusions, suggest that heat supplied from these intrusions was the primary cause of the metamorphic gradient. Metapelites in the contact aureoles surrounding the Nelson and Bonnington intrusions (Pattison and Vogl 2005) contain mineral assemblages that reveal a gradational variation in exposed pressure (depth) of contact metamorphism, ranging from 3.5 to 4.0 kbar in the east of the study area to 2.5–3.0 kbar in the west (Pattison and Vogl 2005).

## Metamorphic assemblages and textures

### Flin Flon arc assemblage

Figure 1b shows a map of regional isograds for the Flin Flon area based on a suite of over 600 thin sections, predominantly from the Hidden and Louis Formations (see electronic supplementary information, Table S1, for coordinate locations). Remnants of igneous mineralogy are rarely preserved above prehnite–pumpellyite facies conditions. However, relict igneous textures such as pseudomorphed phenocrysts (e.g., clinopyroxene and plagioclase) and amygdules are abundant within the Flin Flon metabasites up to lower-amphibolite facies. An important feature of the Flin Flon metabasites is that the rocks rarely show post-metamorphic deformational fabrics, allowing for the preservation of quite complex intergrowth textures between coexisting metamorphic minerals.

Five regional metamorphic mineral isograds were identified in the Flin Flon area (Fig. 1b). These comprise, from S to N: actinolite-in, coincident prehnite-out and pumpellyite-out, hornblende-in, oligoclase-in and actinolite-out. This study focuses on the part of the sequence that spans the middle-greenschist-to-lower amphibolite facies and contains the hornblende-in, oligoclase-in, and actinolite-out isograds.

### Rossland volcanics

Metamorphic mineral assemblage zones and isograds in the Rossland Volcanics are shown in Fig. 1c, based on examination of over 250 thin sections from basaltic samples, including re-examination of selected samples from the study of Powell and Ghent (1996) (see electronic supplementary information, Table S2, for coordinate locations). The isograds comprise actinolite-in, coincident prehnite-out and pumpellyite-out, hornblende-in, and garnet-in. In contrast to the Flin Flon sequence, there is extensive preservation of original igneous mineralogy, particularly of clinopyroxene, amphibole and plagioclase phenocrysts, up to lower-amphibolite facies.

The area of focus for this paper lies between the Bonnington pluton and the ‘tail’ of the Nelson batholith, shown in Fig. 1c, and is composed of a central core area of greenschist facies metamorphism, surrounded by amphibolite facies metamorphic zones marginal to the Bonnington and Nelson plutons. The pattern of isograds in this area and in the region south of the Bonnington and Nelson plutons suggests that metamorphic domains of greenschist facies or higher are the product of elevated temperature resulting from the intrusion of the Nelson and Bonnington

plutons. The ambient pre-intrusion regional metamorphic grade is likely represented south of this area, away from the plutons, where the metamorphic grade is of sub-greenschist facies (maximum grade of prehnite–pumpellyite in metabasites, chlorite zone in metapelites).

### Metamorphic zones and reactions

The salient features of metabasites of the greenschist facies and greenschist–amphibolite transition zone in the Flin Flon and Rossland sequences are described hereafter. Due to the greater sampling density at Flin Flon, and complications arising from the overlapping contact aureoles in the Rossland Volcanics, variations in modal proportions and textures with changing metamorphic grade are more extensively documented in the Flin Flon sequence. Figures 3, 4 and 6 show variations in mineral modes and chemistry with changing metamorphic grade.

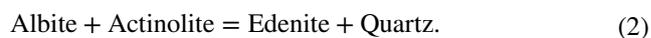
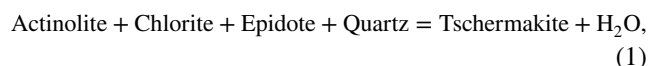
#### Greenschist facies

This zone is characterized in both sequences by the diagnostic assemblage actinolite–albite–epidote–chlorite. In the field, greenschist facies samples consist of a fine-grained, dark green matrix with well-preserved igneous features (e.g., phenocryst pseudomorphs and amygdules). There are no consistent trends in the modal proportions with increasing grade in the greenschist facies and thus variations within mineral modes are primarily a function of different bulk compositions.

#### Hornblende–actinolite zone

The hornblende–actinolite zone is bounded by the hornblende-in isograd (at lower grade) and the oligoclase-in isograd (at higher grade). In Flin Flon, the zone is approximately 3.5 km wide (in a N–S direction), whilst in Rossland the width is variable, most likely due to the effects of overlapping contact aureoles (Fig. 1c). Hornblende is sporadically developed in the lower part of the zone in the Flin Flon sequence and only becomes prevalent approximately 1 km above the hornblende-in isograd.

The production of hornblende is a result of the two major simplified reactions that describe the breakdown of actinolite, albite, chlorite, epidote and quartz to form hornblende. In the reactions below, the hornblende is expressed in terms of its two component end members, tschermakite and edenite (e.g., Cooper 1972; Graham 1974; Laird 1982):

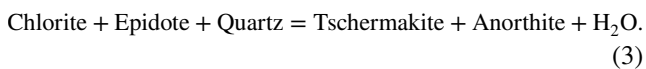


Relative to the greenschist facies samples, the major changes within the Flin Flon sequence may be summarized as: (1) the appearance of hornblende; (2) a slight average increase in the total amphibole content (+2%); (3) a decrease in the average plagioclase modal proportions (−12%) (Figs. 4d, 6b).

### Hornblende–actinolite–oligoclase zone

In the Flin Flon sequence, the hornblende–actinolite–oligoclase zone is marked by the incoming of oligoclase, which coexists with albite and both amphiboles. The development of oligoclase is sporadic within the Rosslund area. It was found in only three samples and thus it was not possible to delineate a clear hornblende–actinolite–oligoclase zone.

In addition to reactions (1) and (2), a third reaction in the greenschist–amphibolite facies transition zone is responsible for producing calcic plagioclase as well as tschermakitic hornblende (e.g., Cooper 1972; Graham 1974):



Modal, textural and compositional analysis from the Flin Flon sequence suggests that the hornblende–actinolite–oligoclase zone is the interval within the greenschist–amphibolite transition zone where the majority of change occurs (Figs. 4, 6). At Flin Flon, these include: (1) the appearance of oligoclase; (2) a decrease in the average albite modal proportion (−13%); (3) a large increase in modal hornblende (+20%); (4) a progressive decrease in the amount of actinolite both as a modal proportion and as a proportion of the total amphibole (−5% on average, with actinolite decreasing to almost zero with increasing grade); (5) an increase in the total amphibole content (+15%); (6) a decrease in chlorite (−5% near the isograd and −11% in the upper parts of the sequence) (Figs. 4, 6).

### Hornblende–oligoclase zone

A small domain within the northernmost outcrops of the Flin Flon sequence contain the actinolite-free assemblage Hbl + Olig + Ab + Ep + Chl + Bt ± Ms + Ilm, north of an actinolite-out isograd. These samples represent the highest grade of metamorphism observed at Flin Flon. The mode of the rocks is dominated by hornblende, plagioclase and epidote, with oligoclase making up over 50% of the total plagioclase content, coexisting with albite.

### Hornblende–calcic plagioclase zone

High grade amphibolite facies samples from the Rosslund suite within the Nelson aureole are completely recrystallized and preserve no igneous mineralogy or textures. Hornblende

and a calcic plagioclase phase (An<sub>50+</sub>) make up most of the rock, with some samples containing small amounts of chlorite, epidote and biotite.

## Mineral chemistry and textures

To better understand the relationships between coexisting minerals and the evolution of continuous and discontinuous reactions across the greenschist–amphibolite transition zone, samples from Flin Flon and Rosslund were chosen for compositional, modal and textural analysis. Quantitative compositional analysis was performed using wavelength dispersive spectrometry (WDS) on a JEOL JXA-8200 electron microprobe at the University of Calgary. All spot analyses were carried out using an acceleration voltage of 15 kV, a current of 20 nA, and approximate spot size of 5 μm. The fine-grained nature of greenschist and lower amphibolite meta-basalts pose a challenge in identifying mineral assemblages, obtaining accurate modal data and assessing the textures between intergrown minerals. In this study, mineral proportions were produced by digitally overlaying multiple X-ray element distribution maps in which different minerals had unique attributes. These maps were then analysed using the program JMicrovision, using colour intensity thresholding, that allowed identification of mineral modes.

## Amphibole textures

### Flin Flon suite

A range of textures was found between actinolite and hornblende, many of which have been reported in earlier studies (e.g., Klein 1969; Graham 1974; Tagiri 1977; Begin and Carmichael 1992). These include: (1) individual homogeneous actinolite and hornblende grains; (2) patchy intergrowths of two coexisting amphiboles with complex irregular grain boundaries (Fig. 2a–c); (3) defined intergrowths distinguished by two amphibole phases being separated by regular sharp grain boundaries that in some case form euhedral rhomb-shaped intergrowths; (4) core-rim structures characterized by actinolite cores surrounded by hornblende (Fig. 2d). High-resolution BSE imaging and compositional mapping revealed no evidence for exsolution between coexisting amphiboles.

The majority of samples containing coexisting actinolite and hornblende show more than one textural variety, with patchy and defined intergrowths occurring in virtually all samples. Analysis of BSE images and compositional maps suggests that the vast majority of coexisting amphiboles occur as intergrowths as opposed to individual grains. Despite the variability, some overall changes in texture were observed with changing grade. Samples

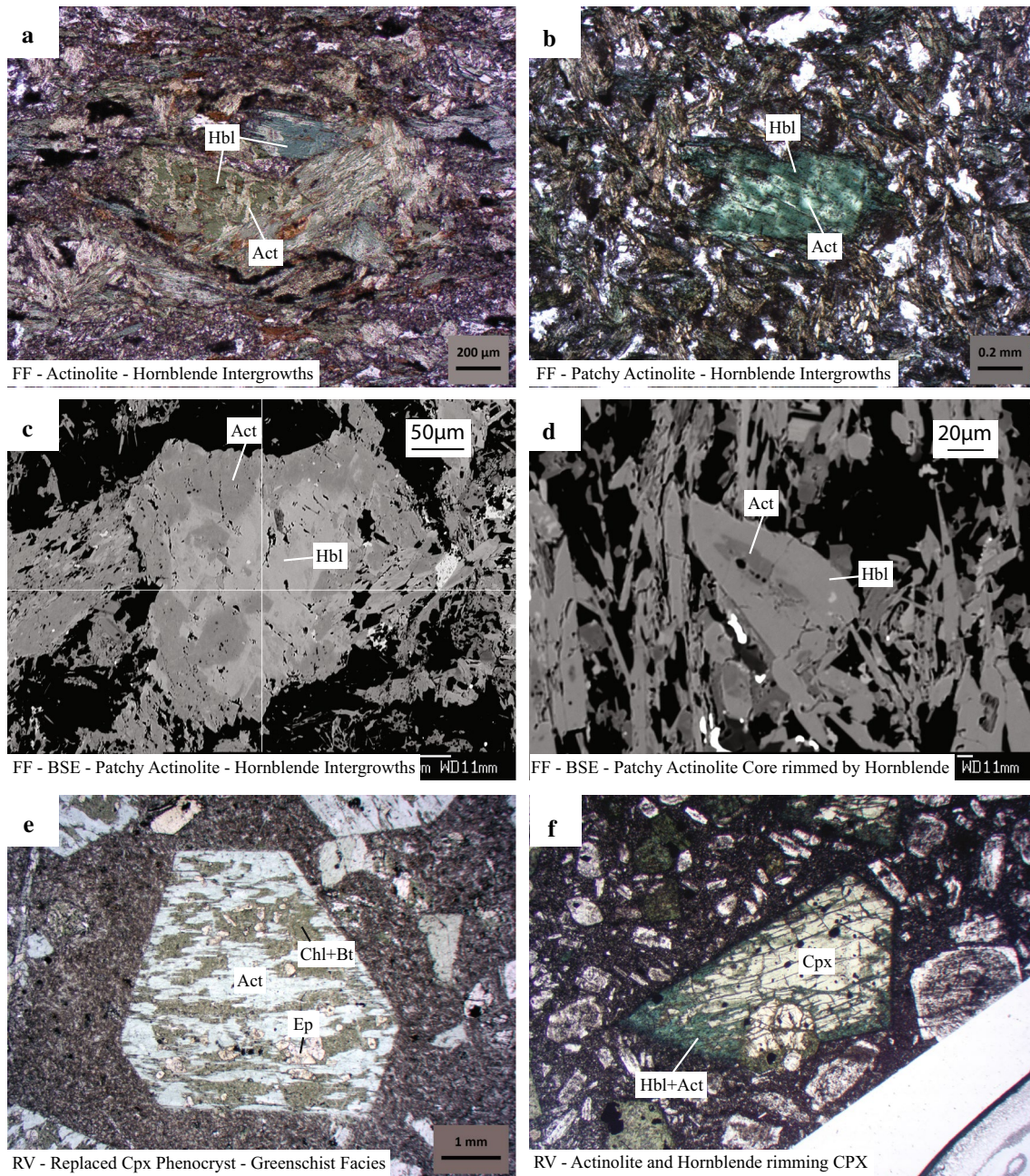


**Fig. 2** Thin section photos: actinolite–hornblende relationships. *FF* Flin Flon sequence, *RV* Rosslund Volcanic sequence. **a** Actinolite–hornblende intergrowths: dark blue-green hornblende with pale green actinolite; **b** very patchy actinolite and hornblende within a clinopyroxene pseudomorph; **c** Back-scattered electron (BSE) image showing

patchy actinolite (dark) and hornblende (light) with sharp irregular contacts; **d** BSE image of patchy actinolite core (dark) surrounded by hornblende (light); **e** euhedral clinopyroxene phenocryst pseudomorphed by actinolite, epidote, chlorite and biotite; **f** Hornblende and actinolite rimming relic clinopyroxene

located just above the hornblende-in isograd contain only minor amounts of hornblende that forms small ‘blebs’ within larger actinolite grains and are interpreted as representing incipient growth of hornblende. Hornblende becomes more abundant moving up-grade, particularly above the oligoclase-in isograd, where patchy and defined

intergrowths become common. The most northerly samples below the actinolite-out isograd contain hornblende as the dominant amphibole and core-rim microstructures (actinolite rimmed by hornblende) dominate, though patchy grains are also still present.

## Rossland volcanics suite

Metamorphic amphiboles in the Rossland Volcanics occur both as replacement of clinopyroxene and amphibole phenocrysts, commonly forming rims around the remnant igneous mineral (Fig. 2f), and as smaller grains within the matrix. Patchy intergrowths are the dominant microstructure involving coexisting amphiboles, both within the matrix and phenocryst pseudomorphs, whilst defined intergrowths and core-rim textures were less common than at Flin Flon.

## Amphibole compositions

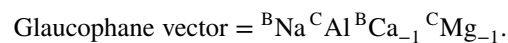
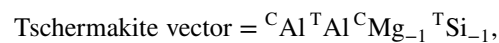
The general structural formula for amphibole group minerals (e.g., Leake et al. 1997; Hawthorne and Oberti 2007; Hawthorne et al. 2012) is:



The C site can be further divided based on crystallographic sites ( $C_5 = (M1)_2(M2)_2(M3)_1$ ) and may comprise a variety of different divalent (Mg,  $Fe^{2+}$ ,  $Mn^{2+}$ ), trivalent (Al,  $Fe^{3+}$ ,  $Mn^{3+}$ ) and tetravalent (Ti) cations (e.g., Leake et al. 1997; Hawthorne and Oberti 2007). Two of the five total C sites (M2) show a strong preference for trivalent cations (e.g., Leake et al. 1997; Hawthorne and Oberti 2007). A number of previous papers describe methods for estimating  $Fe^{3+}$  content within amphiboles based on stoichiometric constraints (e.g., Droop 1987; Holland and Blundy 1994; Schumacher 1997). To assess the influence of uncertainties in the ferric iron estimation, the following methods were tested: (1) minimum, maximum and average recalculation factors of Holland and Blundy (1994); (2) minimum, maximum and average recalculation factors of Schumacher (1997). Recalculating the site allocations using the minimum and maximum recalculation factors was used to generate the lower and upper bounds of the possible ferric iron ratios and assess the effects of the full possible range of ferric iron variation on the important site allocations. These tests suggest that the uncertainty in the site placements is small compared to the observed natural variation for the majority of important cations (< 0.1 cations per formula unit (cpfu) comparing calculated cpfu values for the maximum and minimum possible ferric iron content). The uncertainty is more significant (> 0.1 cpfu) compared to the natural variation for several site placements ( ${}^CFe^{3+}$ ,  ${}^CFe^{2+}$ ,  ${}^BNa$ ) and thus analysing trends in these cations was done with caution. Based on this analysis, it was shown that the compositional trends described in this paper are largely independent of the choice of ferric iron recalculation factor. All amphibole data in plots and tables presented in this paper use ferric iron and cations per formula unit (cpfu) values calculated using an average

recalculation factor following the method of Schumacher (1997) and following the naming recommendations of Leake et al. (1997) and Hawthorne et al. (2012). All analyses were tested using a number of critical stoichiometric criteria to discard poor (non-stoichiometric) analyses (e.g., Schumacher 1997).

Variations in calcic amphibole composition are manifested predominantly through changes in A, B and T cation assemblages. These can be described in terms of both coupled cation exchanges (e.g., tschermakite, edenite and glaucophane substitutions) and homovalent exchanges. Schumacher (2007) described five principal coupled substitution vectors for amphiboles, three of which are relevant to calcic amphiboles and can be expressed in the simplified system  $Na_2O-CaO-MgO-Al_2O_3-SiO_2-H_2O$  as:



These vectors are not linearly independent as can be seen from the formulae above. In the case of the tschermakite substitution, we can calculate the magnitude of the substitution vector, knowing that the total observed  ${}^TAl$  substitution is equal to the sum of the  ${}^TAl$  contributions from the tschermakite ( ${}^TAl_{Tsch}$ ) and edenite ( ${}^TAl_{Ed}$ ) substitutions (i.e.,  ${}^TAl = {}^TAl_{Tsch} + {}^TAl_{Ed}$ ). Given that the  ${}^TAl$  substitution is 1:1 linearly proportional to the  ${}^ANa$  substitution along the edenite substitution vector we can calculate the  ${}^TAl_{Ed}$  ( ${}^TAl_{Ed} = {}^ANa$ ) and  ${}^TAl_{Tsch}$  components ( ${}^TAl_{Tsch} = {}^TAl - {}^TAl_{Ed} = {}^TAl - {}^ANa$ ) (Schumacher 2007). Thus, the magnitude of the three major coupled substitutions relative to an end-member tremolite composition can be calculated using the following formulae for the simplified system  $Na_2O-CaO-MgO-Al_2O_3-SiO_2-H_2O$  (Schumacher 2007):

$$Tsch = {}^TAl - {}^ANa,$$

$$Ed = {}^ANa,$$

$$Gl = {}^BNa.$$

These calculations can be applied more generally to a full chemical system:

$$Tsch = {}^TAl - {}^ANa - {}^AK - 2{}^ACa,$$

$$Ed = {}^ANa + {}^AK + {}^ACa,$$

$$Gl = {}^BNa.$$

A compositional difference between two amphiboles can be described in terms of these vectors as the difference in Tsch (e.g.,  $Tsch_{Hbl} - Tsch_{Act}$ ), Ed (e.g.,  $Ed_{Hbl} - Ed_{Act}$ ) and Gl contents (e.g.,  $Gl_{Hbl} - Gl_{Act}$ ) between coexisting amphiboles. In addition to these coupled substitutions, the

main homovalent exchanges observed between the calcic amphiboles, actinolite and hornblende, are  $\text{Mg}^{2+} \rightleftharpoons \text{Fe}^{2+}$ ,  $\text{Al}^{3+} \rightleftharpoons \text{Fe}^{3+}$ ,  $\text{Al}^{3+} \rightleftharpoons [\text{Fe}_{0.5}\text{Ti}_{0.5}]^{3+}$ .

### Flin Flon suite

Amphibole analyses were acquired from 64 basaltic samples spanning the middle-greenschist-to-lower amphibolite facies, including 30 samples containing coexisting actinolite and hornblende (see electronic supplementary information, Table S3, for a complete set of representative and average

amphibole compositions). Figure 3 shows a selection of amphibole data from the Flin Flon sequence plotted on a set of amphibole compositional plots. Whilst there is some scatter in the data, there is a clear grouping into two sets of compositions, separated by a compositional gap. For ease of terminology, these two groupings are loosely termed ‘actinolite’ and ‘hornblende’. The compositional gap going from actinolite to hornblende is characterized by an increase in A-site occupancy,  $^{\text{C}}\text{Al}$ ,  $^{\text{C}}\text{Ti}$ ,  $^{\text{C}}\text{Fe}^{3+}$  and  $^{\text{B}}\text{Na}$ , with a corresponding decrease in  $^{\text{T}}\text{Si}$ ,  $\text{Mg}^{2+}/\text{Mg}^{2+}+\text{Fe}^{2+}$  and  $^{\text{B}}\text{Ca}$ . The data are also expressed in terms of the coupled substitution

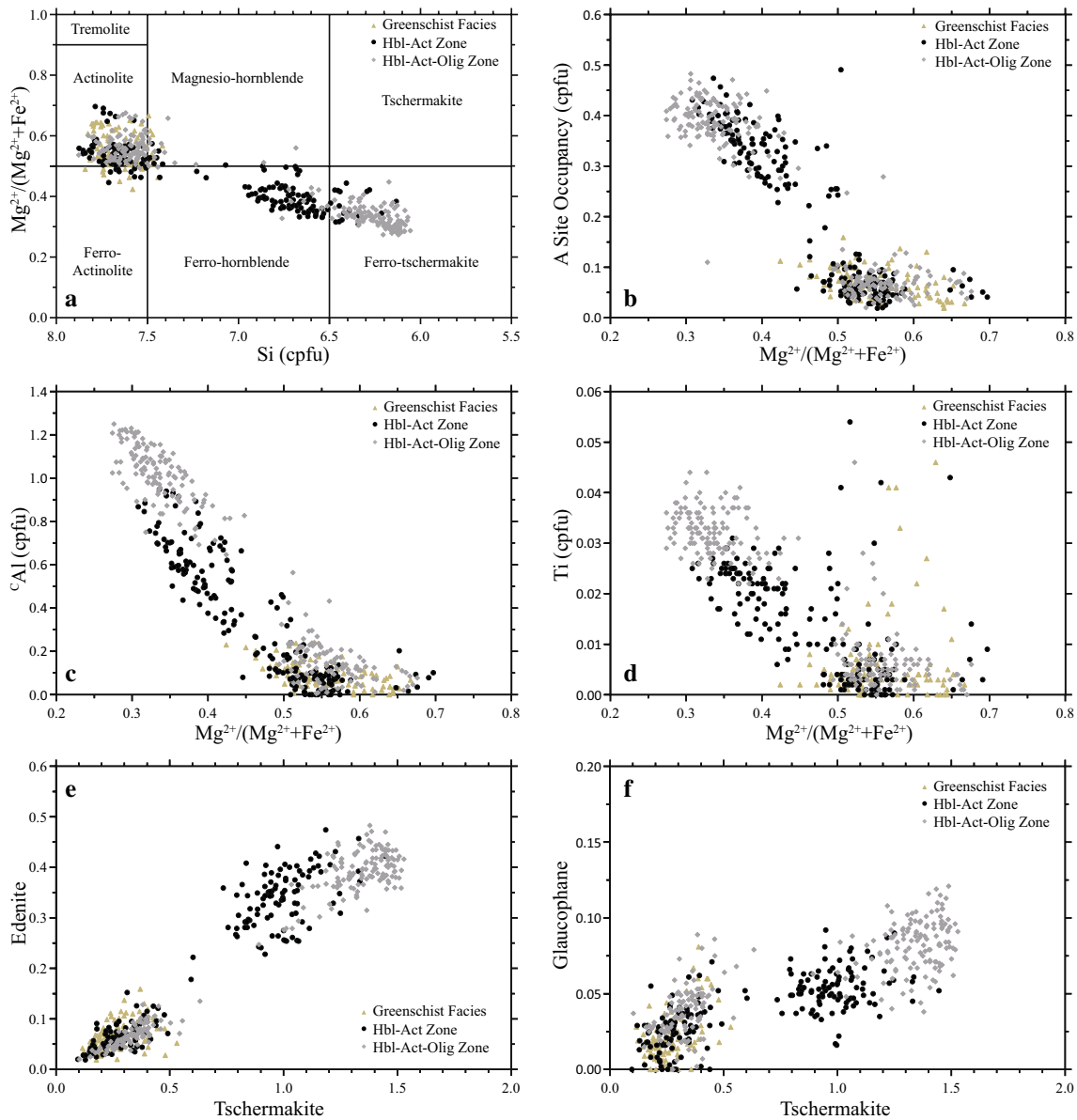


**Fig. 3** Amphibole compositional diagrams for Flin Flon data grouped according to metamorphic zone (greenschist facies, hornblende–actinolite zone and hornblende–actinolite–oligoclase zone). See text explanation of calculation of cations per formula unit (cpfu) (after

Schumacher 1997) and derivation of exchange vectors (after Schumacher 2007). Fields for the calcic amphibole classification plot after Leake et al. (1997)

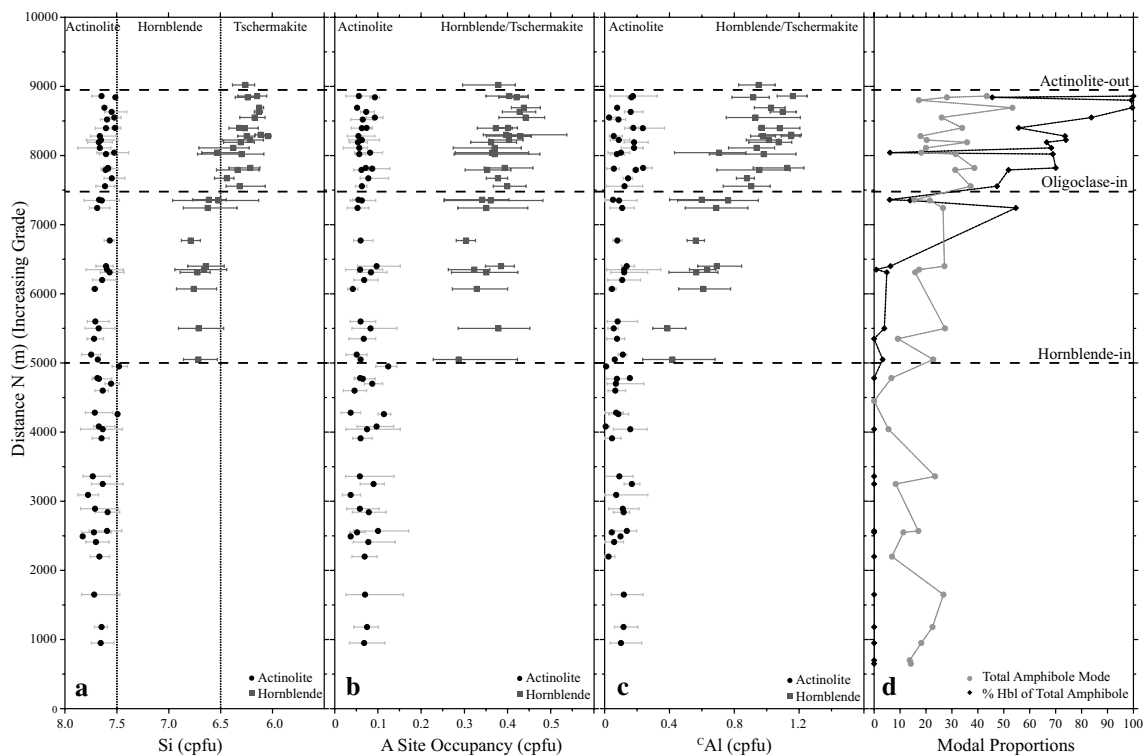


**Fig. 4** Flin Flon amphibole composition and modal plots versus grade. Si (**a**), A-site occupancy (**b**),  $^C\text{Al}$  (**c**), and modal proportions (**d**) plotted versus distance north (m) (taken as a proxy for grade—see text for discussion). The points represent the average composition for

that sample whilst the lines represent the full range of compositions observed. The positions of the mineral isograds (hornblende-in, oligoclase-in and actinolite-out) are shown by the dashed lines. Compositional fields for amphibole after Leake et al. (1997)

vectors (Fig. 3e, f) which shows a tight grouping of actinolite compositions, compared to hornblende which shows a greater spread and is characterized by higher tschermakite and edenite components and slightly higher glaucophane content.

To identify changes in the composition of actinolite and hornblende with changing grade, the data are divided into three series based upon the metamorphic zone in Fig. 3: (1) greenschist facies (actinolite-only); (2) hornblende–actinolite zone; (3) hornblende–actinolite–oligoclase zone. In addition, key amphibole compositional parameters (Si, A-site occupancy and  $^C\text{Al}$ ) and amphibole modal proportions were plotted versus the geographical positioning along a N–S transect at a high angle to the E–W oriented isograds, to identify changes in composition with grade (Fig. 4). The graphs show there is no significant variation in the composition of the actinolite with changing grade. By contrast, the hornblende shows a distinct shift towards more tschermakitic compositions that occurs abruptly across the oligoclase-in isograd, resulting in a divergence in the compositions of actinolite and hornblende. The increase in the size of the compositional gap across the oligoclase-in isograd is largest in terms of the  $^T\text{Si}$ ,  $^C\text{Al}$ , and  $^C\text{Ti}$  contents whilst a less distinct change in the A-site occupancy is observed

(Figs. 3, 4). Hornblende compositions above the actinolite-out isograd, are the same as those just below the actinolite-out isograd (Fig. 4).

The average compositional gap between actinolite and hornblende expressed in terms of the difference in Tsch ( $\text{Tsch}_{\text{Hbl}} - \text{Tsch}_{\text{Act}}$ ), Ed ( $\text{Ed}_{\text{Hbl}} - \text{Ed}_{\text{Act}}$ ) and Gl contents ( $\text{Gl}_{\text{Hbl}} - \text{Gl}_{\text{Act}}$ ) is given in Table 1 for both the hornblende–actinolite and hornblende–actinolite–oligoclase zones. These data indicate there is also a small change in the orientation of the vector describing the compositional divide characterized by a larger increase in the Tsch content relative to the change in Ed content across these two zones (Table 1; Fig. 3e). A noticeable increase in the modal proportions of amphibole (combined actinolite and hornblende) and a large increase in the relative proportion of hornblende is observed going from the hornblende–actinolite zone to hornblende–actinolite–oligoclase zone.

### Rosslund volcanics suite

Amphibole analyses were obtained from 24 basaltic samples spanning the greenschist-to-upper amphibolite facies. The samples can be broadly divided into two types based upon the textures and compositions of the amphiboles (Fig. 5).

**Table 1** Summary of amphibole data from the literature and this study

Paper name	Grade	Textural description	Plagioclase	Equilibrium?	Analyses	Exchange vectors		
						Tsch	Ed	Gl
FF—Average Hbl—Act Zone		C–R, RInt, IrInt	Ab; Olig	Y	1265A	0.69	0.27	0.03
FF—Average Hbl—Act—Olig Zone		C–R, RInt, IrInt	Ab; Olig	N		0.97	0.31	0.04
RV—Average clustered data		C–R, RInt, IrInt	Ab; Olig	Y	381A	0.68	0.41	0.03
Allen and Goldie (1978)	G–A	IC, C–R, RInt, IrInt	–	Y	10A; 5P	0.40	0.20	0.06
Begin and Carmichael (1992)	G–A to UA	Rint, C–R	Ab; Olig	Y	8A; 4P	0.85	0.36	0.06
Brady (1974)	St-Ky Zone	IrInt	Olig; And	Y	24A ; 12P	0.70	0.34	0.04
Cooper and Lovering (1970)	G–A (MP)	EL <sup>a</sup> , C–R	Ab; Olig	Y	10A; 2P	0.86	0.27	–0.02
Maruyama et al. (1983)	G–A (MP)	IC, C–R	Ab; Olig	Y	9A; 2P	0.37	0.16	0.15
Sampson and Fawcett (1977)	G–A	C–R	Ab; Olig; And	N	24A; 6P	1.06	0.27	0.10
Terabayashi (1993)	G–A (LP)	Int; C–R	Olig	Y	18A; 3P	0.48	0.22	0.01
Choudhuri (1974)	G–A (LP)	C–R	–	Y	11A; 3P	0.87	0.14	0.09
Hietanen (1974)	G–A (LP)	C–R, IrInt	Ab-An	Y	29A; 0P	No pairs		
Misch and Rice (1975)	GS–UA (MP)	No coexisting	Ab; Olig	Y	22A; 0P	No pairs		
Tagiri (1977)	G–A to UA (MP)	RInt, IrInt	Ab; Olig	Y	23A; 5P	0.81	0.32	0.02
Bucher-Nurminen (1982)	UA	C–R	–	Y	8A; 1P	0.77	0.49	–0.04
Compton (1958)	GS; G–A; A	C–R; IrInt	–	N	5A; 0P	No Pairs		
Grapes (1975)	G–A	C–R; IrInt	–	N	26A; 11P	0.38	0.42	–0.01
Smelik et al. (1991)	Amphibolite	EL	–	Y	16A	0.74	0.35	–0.15
Klein (1969)	Mixture	IrInt; IC	–	Y	14A; 7P	0.65	0.20	0.08
Graham (1974)	G–A (MP)	C–R; IrInt	Ab	N	19A; 5P	0.31	0.28	0.12
Boyle (1986)	G–A (MP)	C–R	Ab; Olig	Y	8A; 4P	0.56	0.32	0.02
Yamaguchi (1985)	Igneous	Int	–	Y	9A; 0P	No pairs		

The calculated compositions ('Exchange Vectors') describe the average compositional gap between actinolite and hornblende. The average compositional gap is expressed in terms of the difference in Tsch ( $Tsch_{Hbl} - Tsch_{Act}$ ), Ed ( $Ed_{Hbl} - Ed_{Act}$ ) and Gl contents ( $Gl_{Hbl} - Gl_{Act}$ ) between the coexisting actinolite and hornblende. For the literature data, this average only includes actinolite–hornblende pairs that occur within the same sample (and usually grain)

G–A greenschist–amphibolite transition zone, UA upper amphibolite, GS greenschist, MP medium pressure (Barrovian-type), LP low pressure (Buchan-type), C–R core–rim, RInt regular intergrowths, IrInt irregular intergrowths, EL exsolution lamellae, IC individual crystals, A total number of analyses; P number of actinolite–hornblende pairs

<sup>a</sup>Exsolution lamellae of Cooper and Lovering (1970) were later reinterpreted to be fine-twinning planes

The first group has two distinct populations of amphibole observed in BSE images and compositional data that cluster into either actinolite or hornblende compositions separated by a distinct compositional gap (referred to as Group 1 amphiboles in Fig. 5). The second contains patchy amphiboles that show no consistent break in composition between actinolite and hornblende (Group 2 amphiboles).

There is considerably more scatter in the size of the compositional gap within the Group 1 Rosslund samples as compared to the Flin Flon suite, particularly in terms of the Mg/Fe ratio, the A-site occupancy and the <sup>C</sup>Al content (Fig. 5). An average vector describing the compositional gap between actinolite and hornblende (Table 1) suggests that it is similar to that of the Flin Flon sequence but is characterized by a greater proportion of edenite exchange relative to tschermakite and glaucophane.

BSE imaging of Group 2 samples demonstrates that amphibole grains are irregular and patchy rather than showing continuous zonation. The backscatter intensity varies between different patches suggesting a scatter in composition rather than separation into two distinct amphibole phases, consistent with the quantitative compositional data (Fig. 5). Many of the 'hornblende' grains from these Group 2 samples have compositions that fall within the compositional gap observed within the Group 1 samples and the Flin Flon suite.

## Plagioclase textures and compositions

### Flin Flon suite

Plagioclase group minerals were analysed in 40 samples from Flin Flon, 19 of which come from within the

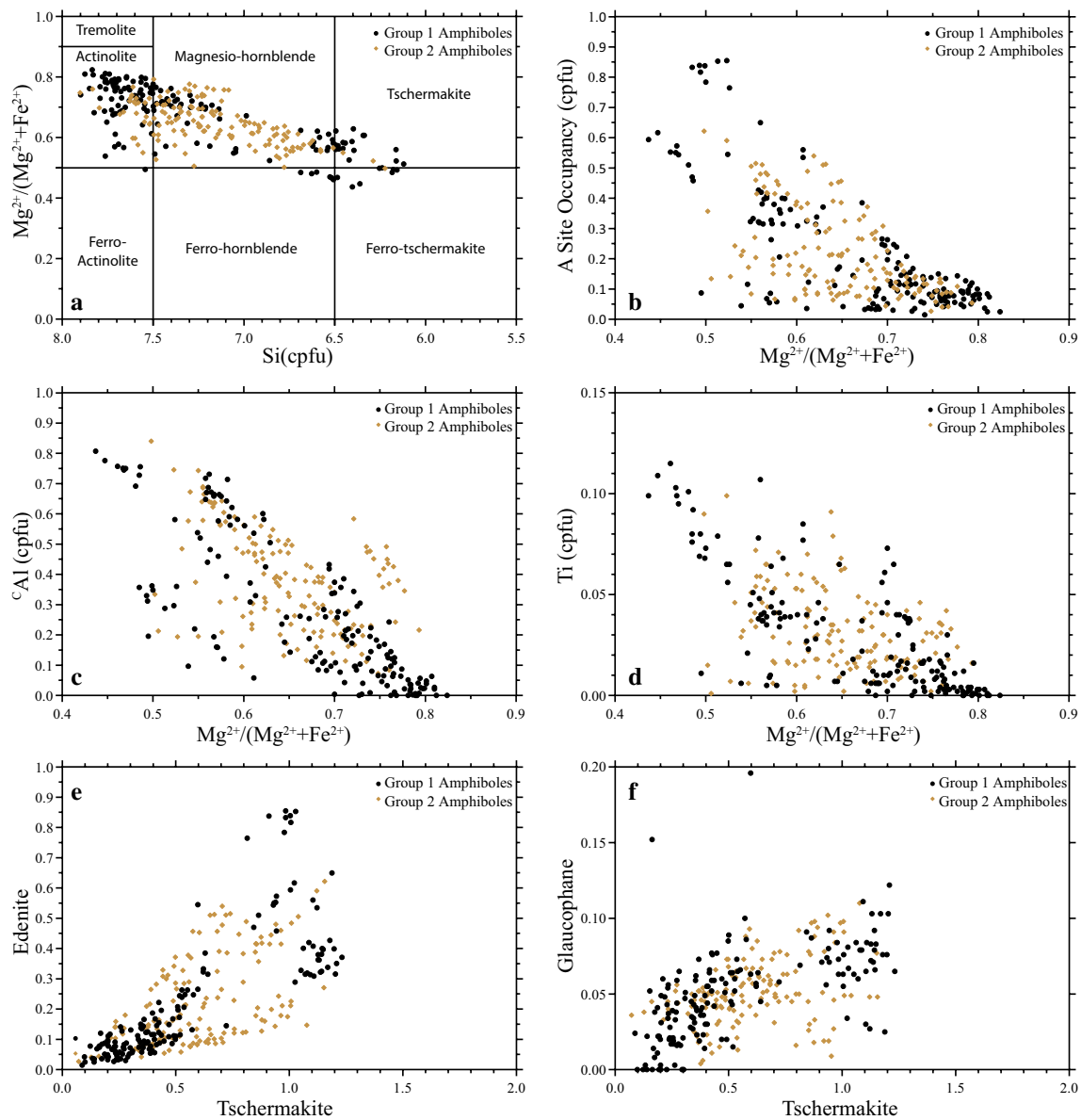


**Fig. 5** Amphibole compositional diagrams for the Rosslund Volcanic data grouped according to amphibole type (see text for definition). See text explanation of calculation of cations per formula unit (cpfu)

(after Schumacher 1997) and derivation of exchange vectors (after Schumacher 2007). Fields for the calcic amphibole classification plot after Leake et al. (1997)

hornblende–actinolite–oligoclase zone (see electronic supplementary information, Table S4, for a complete set of average plagioclase compositions). The anorthite content [ $An = Ca/(Ca + Na + K)$  in cpfu] and modal proportions are plotted with respect to grade in Fig. 6. Within the greenschist facies and the hornblende–actinolite zone, albite is the only plagioclase present and has an average modal proportion of 43% in the greenschist facies decreasing to 30% in the hornblende–actinolite zone. The albite in these zones shows some variation in composition between  $An_{0.8-9.9}$  with an average of  $An_{4.1}$  in these zones.

Above the oligoclase-in isograd, within the hornblende–actinolite–oligoclase zone, albite and oligoclase coexist variously as both fine intergrowths and as separate grains that commonly share grain boundaries. A distinct compositional gap separates albite (average:  $An_{3.2}$ ; range:  $An_{1.1-5.8}$ ) from oligoclase (average:  $An_{22.3}$ ; range:  $An_{17.5-26.0}$ ). There is no evidence for the gap closing with increasing grade, with albite compositions showing limited compositional variation and oligoclase shifting slightly towards more calcic compositions. Within the highest grade samples, in the upper part of the

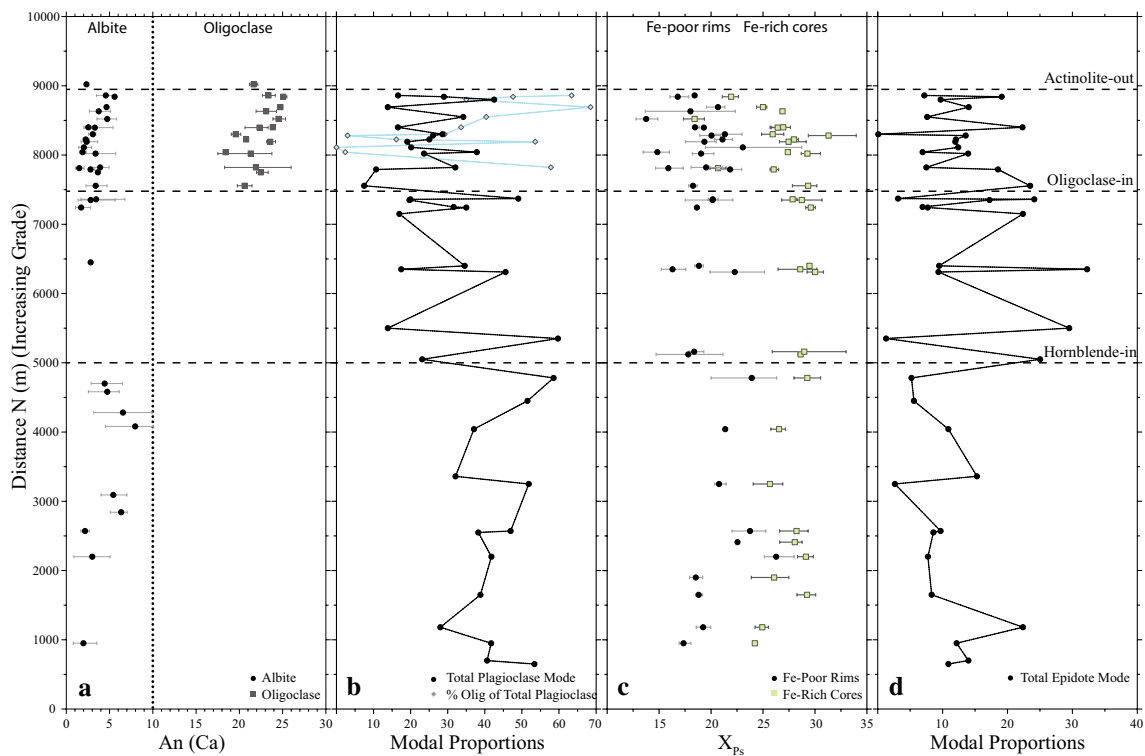


**Fig. 6** Flin Flon plagioclase and epidote compositions and modes plotted versus distance N (proxy for increasing grade). For compositional plots (**a**, **c**), the points represent the average compositions, whilst the lines indicate the range of compositions. The epidote com-

positions are expressed in terms of the  $X_{Ps}$  content [ $X_{Ps} = 100(\text{Fe}^{3+}/(\text{Al} + \text{Fe}^{3+}))$ ]. The points within the modal plots indicate the determined modal proportions for plagioclase (**b**) and epidote (**d**)

hornblende-actinolite-oligoclase and hornblende-oligoclase zones, albite comprises 30–40% of the total plagioclase.

### Rossland volcanics suite

In contrast to the Flin Flon sequence, preservation of igneous plagioclase is common in greenschist-to-lower amphibolite facies samples. Most metamorphic plagioclases within the greenschist facies and lower amphibolite facies (hornblende-actinolite zone) occur as rims around primary igneous plagioclase phenocrysts and as patchy replacement of matrix grains.

Within greenschist and lower amphibolite facies zones, the majority of samples contain metamorphic albite with compositions showing some variation between  $\text{An}_{1-8}$ . Four samples from the hornblende-actinolite-oligoclase zone are interpreted to contain coexisting albite and oligoclase, the two minerals occurring as separate individual matrix grains or more rarely as patchy intergrowths within the matrix. In these samples, there exists a distinct gap in composition between the albite and oligoclase grains. Both the albite and oligoclase grains show some variation in compositions with albite varying from  $\sim \text{An}_1$  to  $\text{An}_8$  and oligoclase between  $\sim \text{An}_{20}$  and  $\text{An}_{39}$ . Metamorphic plagioclase occurring within

the higher grade amphibolite facies samples is considerably more calcic, with compositions varying between  $\text{An}_{43}$  and  $\text{An}_{95}$ . Due to the irregular development of oligoclase within the Rossland meta-basalts, it was not possible to define an oligoclase-in isograd.

### Epidote textures and compositions

Compositional variation within epidote group members is mostly the result of the exchange of  $\text{Fe}^{3+}$  and Al, though other possible exchanges include  $\text{Mn} \rightleftharpoons \text{Al}$ ,  $\text{Fe}^{3+}$  and  $\text{Ca}^{2+}\text{Fe}^{3+} \rightleftharpoons \text{REE}^{3+}\text{Fe}^{2+}$  (e.g., Franz and Liebscher 2004). Variation in epidote composition is expressed as the  $X_{Ps}$  content ( $X_{Ps} = 100(\text{Fe}^{3+}/(\text{Al} + \text{Fe}^{3+}))$ ); often referred to as the pistacite content).

### Flin Flon suite

Epidote is an important component of the Flin Flon suite and is ubiquitous from prehnite-pumpellyite to amphibolite facies. It is usually found as euhedral-subhedral grains or granular aggregates in the matrix (Fig. 7a, c, d) and as individual grains within clinopyroxene phenocrysts. BSE imaging of epidote grains shows that most have a relatively

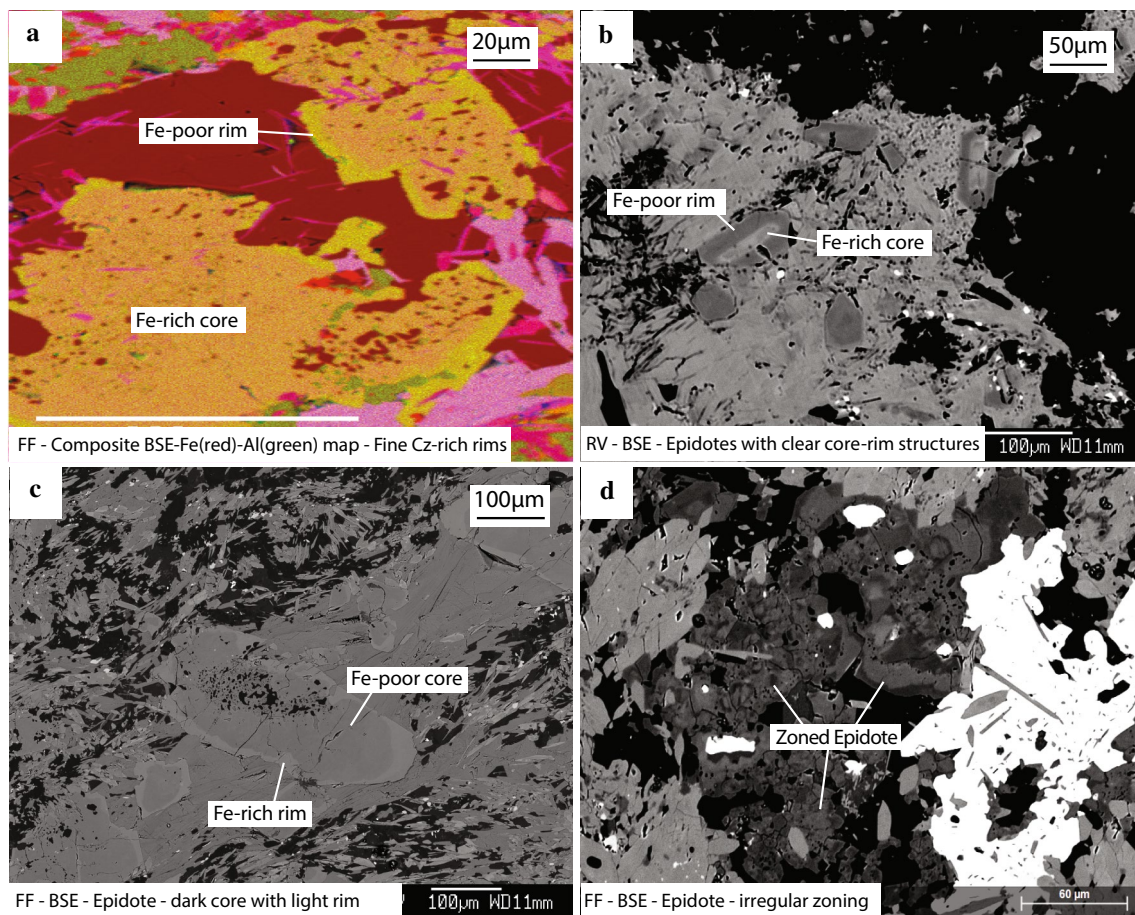


**Fig. 7** BSE images of epidote within the Flin Flon (FF) and Rossland Volcanic (RV) sequences. **a** Fe and Al X-ray compositional maps overlain on BSE image (lighter yellow areas represent Fe-poor

epidote domains) (FF); **b** Epidote with clear core (Fe-rich) and rim (Fe-poor) structures (RV); **c** Reverse zoning with Fe-rich rim (FF); **d** Irregular zoning within epidote (FF)

light-coloured (Fe-richer) core surrounded by a darker (Fe-poorer) rim (Fig. 7a, b). More complex, irregular zonation (Fig. 7d), and zoning with the opposite compositional direction (dark core; light rim) (Fig. 7c), are observed in some samples. Figure 6c shows the variation with grade of  $X_{Ps}$  for core and rim areas of epidote grains from 36 samples (426 analyses—see electronic supplementary information, Table S5, for a complete set of average epidote compositions). Epidote cores are Fe-richer (mean  $X_{Ps} = 27.8$ ; range 24–32) than the rims (mean  $X_{Ps} = 19.3$ ; range 17–24). A compositional gap between epidote cores and rims is present in most samples, though the width and absolute value of the gap varies irregularly going up grade (Fig. 6c).

#### Rossland volcanics suite

Epidote is generally a minor component in the meta-basalts of the Rossland Volcanics suite, and is mainly developed in the greenschist and lower amphibolite facies. Like at Flin Flon, some epidote grains contain Fe-rich cores with

Fe-poor rims (Fig. 7b). However, the more Fe-rich compositions observed within the Flin Flon sequence are absent within the Rossland sequence. Epidote from the greenschist and lower amphibolite facies ranges in composition from  $X_{Ps} = 19$ –26, whilst epidote in higher grade samples is Fe-poorer (range of  $X_{Ps} = 12$ –17).

### Comparison of textures and compositions from other sequences

#### Coexisting calcic amphiboles

Textures and compositions of coexisting actinolite and hornblende described from the literature are summarized in Table 1, and are similar to those seen at Flin Flon and Rossland. The most common textures observed are irregular, patchy amphibole intergrowths and core-rim microstructures between the coexisting amphiboles (e.g., Sampson and Fawcett 1977; Brady 1974; Graham 1974; Maruyama et al.

1983) (Table 1). Few studies documented changes in textures with increasing grade, a prominent exception being Begin and Carmichael (1992), who described an evolution from epitaxial intergrowths of actinolite and hornblende down-grade of the oligoclase-in isograd to core and rim structure above it. Exsolution microstructures involving actinolite and hornblende have not been described with the exception of Smelik et al. (1991). Using analytical electron microscopy (AEM), they described very fine (5–15 nm) exsolution lamellae of actinolite in hornblende grains.

A total of 253 analyses, including 47 actinolite–hornblende pairs, were compiled from 19 different sequences from the literature, and compared with the new amphibole database from Flin Flon and Rosslund (1646 analyses). Average compositional vectors describing the actinolite–hornblende compositional gap were calculated for all of the sequences (Table 1). Figure 8 shows a comparison of literature data with those from Flin Flon and Rosslund. Whilst there is considerable scatter in the literature data, a clear gap is apparent in terms of the  $^T\text{Si}$  and Tsch contents, the size of which is comparable to that shown in the Flin Flon and Rosslund amphiboles.

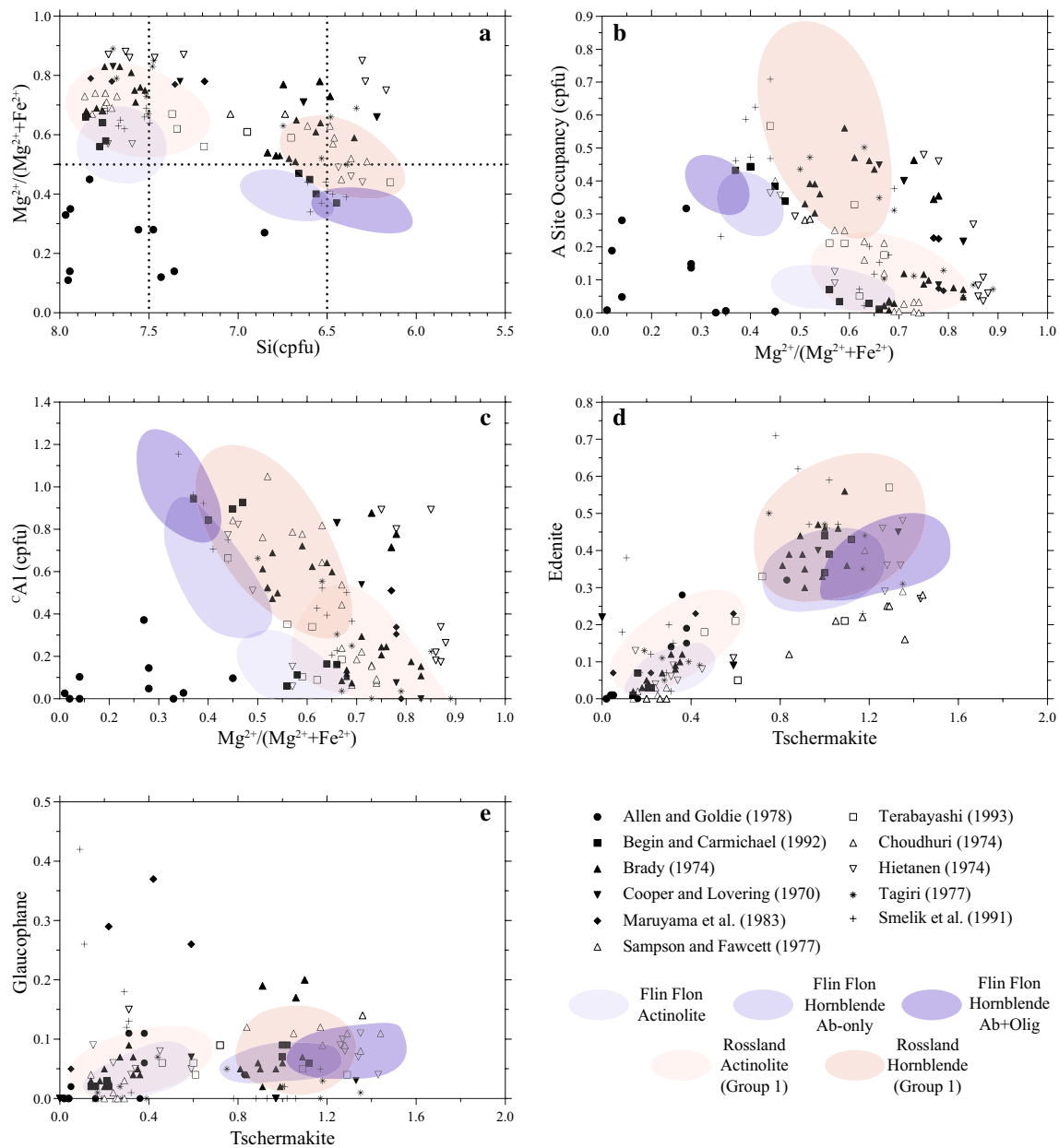


**Fig. 8** Comparison of actinolite–hornblende data from this study and data from the literature. Blue coloured areas represent range of Flin Flon data points; red coloured zones indicate range of Rosslund Volcanics Group 1 amphibole data

A similar compositional gap exists between the orthorhombic amphiboles, anthophyllite and gedrite, with anthophyllite representing an orthorhombic (Fe–Mg) analogue of actinolite and gedrite representing an orthorhombic (Fe–Mg) equivalent of hornblende. A number of authors have noted that this compositional gap is characterized by a similar difference in the degree of tschermakite and edenite substitution as in the actinolite–hornblende gap (e.g., Robinson 1982; Schumacher 2007). Figure 9 compares compositions from anthophyllite–gedrite pairs from seven papers (Spear 1980; Stout 1972; Schneiderman and Tracy 1991; Smelik and Veblen 1993; Frimmel 1996; Janák et al. 1999; Champness and Rodgers 2000) with the actinolite–hornblende data from this study and from the literature, showing the similarity in the size and nature of the compositional gap. The anthophyllite–gedrite gap is characterized by a smaller Ed and larger Gl component relative to Tsch content. Occurrences of intergrowths of gedrite and anthophyllite interpreted to be exsolution microstructures are described in a number of sequences (e.g., Robinson and Jaffe 1969; Spear 1980; Smelik and Veblen 1993).

## Coexisting plagioclase group minerals

Coexisting albitic plagioclase and oligoclase separated by a distinct compositional gap within transitional greenschist–amphibolite sequences has been widely recognized in the literature. A summary of textures and compositions from these sequences is shown in Table 2. The textures are variable, ranging from individual coexisting crystals of albite and oligoclase, regular and patchy intergrowths, and core-rim microstructures (e.g., Maruyama et al. 1982; Grapes and Otsuki 1983; Ashworth and Evirgen 1985a). Albite cores rimmed by oligoclase represent the most commonly described microstructure, particularly in lower-grade samples just above the oligoclase-in isograd (e.g., Maruyama et al. 1982; Grapes and Otsuki 1983).

Grapes and Otsuki (1983) provided a description of the evolution of plagioclase compositions in quartzofeldspathic schists across the greenschist–amphibolite transition. They found a compositional gap between albite ( $An_{0-1}$ ) and oligoclase ( $An_{20-26}$ ) in biotite zone samples that decreased with increasing grade to compositions of  $An_6$  and  $An_{12}$  in the upper garnet zone. Ashworth and Evirgen (1985a)

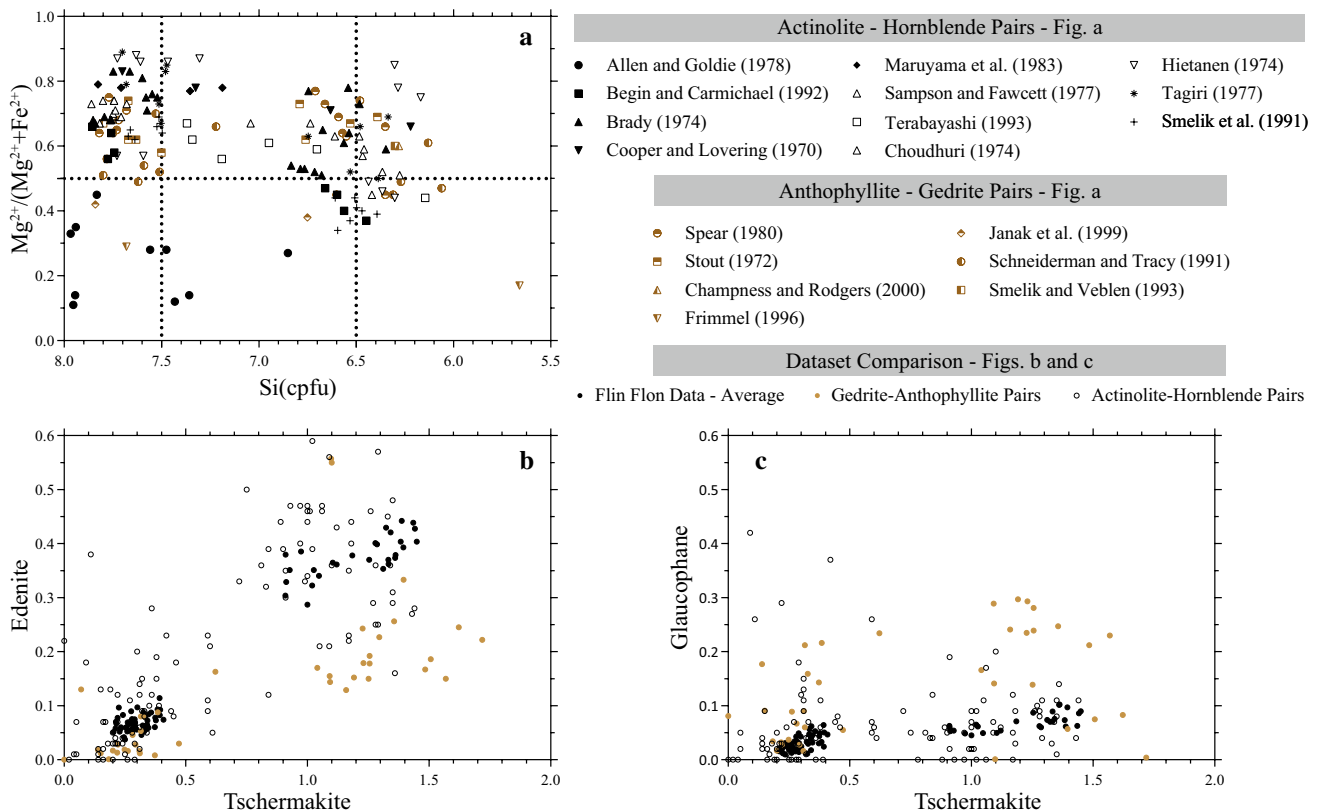


**Fig. 9** Comparison of coexisting actinolite–hornblende (black symbols) and gedrite–anthophyllite data (brown symbols). **a** Literature data for actinolite–hornblende data compared to gedrite–anthophyllite. **b, c** Comparison of actinolite–hornblende data from Flin Flon,

and actinolite–hornblende and gedrite–anthophyllite compositions from the literature, expressed in terms of exchange vectors (tschermakite, edenite, and glaucophane)

**Table 2** Summary of plagioclase textural and compositional data from the literature and this study

Paper name	Location	Protolith	Grade	Textural description	Analyses	Albite	Oligoclase
This study	Flin Flon	Metabasites	Hbl–Act–Olig Zone	IrInt	210A	1–6	18–26
This study	Rosslund Volcanics	Metabasites	G–A transition	IrInt	186A	1–8	20–39
Ashworth and Evirgen (1985a)	Menderes Massif, Turkey	Pelitic	Gt Zone	IrInt; C–R	2P	1–2	19–22
Ashworth and Evirgen (1985a)	Menderes Massif, Turkey	Pelitic	St Zone	IrInt; C–R	1P	1.02	16
Ashworth and Evirgen (1985a)	Menderes Massif, Turkey	Pelitic	St + Ky Zone	IrInt; C–R	2P	0–1	13–15
Grapes and Otsuki (1983)	Southern Alps, New Zealand	Semi-pelite (Qtz-Plag Layers)	Bt Zone (MP)	C–R	–	0.5–0.9	20–24
Grapes and Otsuki (1983)	Southern Alps, New Zealand	Semi-pelite (Qtz-Plag Layers)	Upper Gt Zone (MP)	IC; IrInt	–	1–3	15–20
Grapes and Otsuki (1983)	Southern Alps, New Zealand	Semi-pelite (Mica-rich Layers)	Bt Zone (MP)	IrInt; C–R	–	0–1.5	20–26
Maruyama et al. (1982)	Kasugamura, Japan	Metabasites	G–A transition (MP—low grade)	C–R	–	7–8	25
Maruyama et al. (1982)	Yap Islands	Metabasites	G–A transition (MP—low grade)	C–R	–	3–4	25
Maruyama et al. (1982)	Kasugamura, Japan	Metabasites	G–A transition (MP—med/high grade)	Zoned C–R	–	1–10	13–25
Maruyama et al. (1982)	Yap Islands	Metabasites	G–A transition (MP—med/high grade)	Zoned C–R	Single Grain	3–7	17–29
Cooper (1972)	Haast Schist, New Zealand	Semi-pelite	G–A transition	C–R; IC	–	0–2	22–26
Morteani and Raase (1974)	Eastern Alps, Austria/Italy	Meta-igneous	G–A transition	C–R	–	0–5	15–20
Begin (1992)	Cape Smith Belt, Northern Quebec	Metabasites	G–A transition	C–R	–	3–10	17–21

Listed compositions represent range of reported compositions for albite and oligoclase

*G–A* greenschist–amphibolite transition zone, *MP* medium pressure (Barrovian-type), *LP* low pressure (Buchan-type), *C–R* core-rim, *IrInt* irregular intergrowths, *IC* individual crystals

documented a similar convergence in compositions from a sequence of Barrovian metapelites, with oligoclase compositions evolving from  $An_{19-22}$  in the garnet zone to  $An_{13-15}$  in the staurolite and kyanite zones, with albite compositions showing little variation ( $An_{0-1}$ ). Maruyama et al. (1982) documented a clear compositional gap between albite and oligoclase grains but found that the oligoclase grains were strongly zoned, varying in composition from  $An_{17}$  to  $An_{29}$  in a single grain.

### Coexisting epidote group minerals

A compositional gap in the clinozoisite–epidote series has been noted in a number of prehnite–pumpellyite to lower amphibolite sequences (e.g., Strens 1963, 1964, 1965; Bishop 1972; Hietanen 1974; Raith 1976; Katagas and Panagos 1979; Grapes and Hoskin 2004) as well as in several experimental studies (Strens 1965; Fehr and

Heuss–Aßbichler 1997; Heuss–Aßbichler and Fehr 1997). Reported epidote textures include continuous zonation, core-rim textures, individual grains of clinozoisite and epidote, and lamellae of epidote within clinozoisite (Grapes and Hoskin 2004 and reference therein). Figure 10, modified after Grapes and Hoskin (2004), shows a compilation of literature data highlighting compositional gaps between epidote and clinozoisite (represented by the grey dashed lines), compared to the average compositional gap from Flin Flon (bold black line). The literature data show considerable scatter both in the size and position of the gap. The Fe-poor compositions have  $X_{Ps}$  values ranging between 11–19% whilst the Fe-rich compositions vary between 22–29%. The gap between the average epidote core and rim compositions from the Flin Flon sequence covers a more Fe-rich compositional range than the majority of the compositional gaps from other sequences reported in the literature, but overlaps with them.

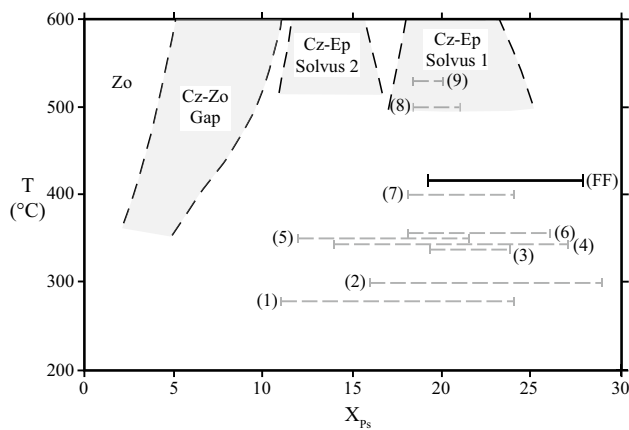


**Fig. 10** Comparison of average epidote compositional gaps (between core and rim) from the Flin Flon sequence with a compilation of data from the literature (modified after Grapes and Hoskin 2004). Grey dashed lines represent compositional gaps within the clinzoisite–epidote series, estimated from various sources within the literature (see Grapes and Hoskin 2004 for discussion). The black complete line represents the gap between the average core and average rim compositions from the Flin Flon sequence. Temperature range for the Flin Flon sequence approximated using thermodynamic modelling. Data sources: (1) Strens (1964); (2) Holdaway (1965); (3) Schreyer and Abraham (1978); (4) Bishop (1972); (5) Hietanen (1974); (6) Katagas and Panagos (1979); (7)–(9): Raith (1976)—increasing grade from (7) to (9). Gap and Solvus Sources: Cz-Zo Gap: Franz and Selverstone (1992); Cz-Ep Solvus 1 and 2: Fehr and Heuss-Aßbichler (1997)

## Discussion

The new data from Flin Flon and Rossland presented in this paper, combined with the data compiled from the literature, represent the most detailed documentation of compositions and textures of coexisting minerals with changing grade within the greenschist and amphibolite facies and across the greenschist–amphibolite facies transition. These data are used to assess the interplay between equilibrium and disequilibrium processes in: (1) the development and evolution of compositional gaps within the amphibole, plagioclase, and epidote mineral series in the greenschist–amphibolite facies transition; (2) the progress of the dominant metamorphic devolatilization reactions that effect this transition; (3) influencing the reliability of using natural datasets to derive miscibility compositional limits.

### Coexistence of multiple phases from the same mineral group

The coexistence of two phases from the same mineral group that have distinctly different compositions (e.g., actinolite–hornblende, albite–oligoclase, epidote–clinzoisite) is a common characteristic of transitional greenschist–amphibolite sequences and of other facies transitions. However,

this coexistence is not, in itself, indicative of an equilibrium relationship, although it has commonly been interpreted as such in many studies. In the context of equilibrium thermodynamics, the term “miscibility gap” is defined as any discontinuity in a solid solution series (e.g., Robinson 1982). The shape of a miscibility gap as a function of temperature and pressure defines whether it classifies as being either a solvus (e.g., Robinson 1982; Zingg 1996) or a transition loop (Maruyama et al. 1983; Terabayashi 1993). The nature of changes in mineral composition with increasing grade may allow these two possibilities to be distinguished, assuming the compositional gaps are controlled by processes occurring at equilibrium. However, disequilibrium processes must also be considered, such as metastable persistence of mineral phases into higher grade domains where the stable phase is of a different composition than the metastable phase.

## Actinolite and hornblende

### Introduction

Many authors have interpreted the compositional gap between actinolite and hornblende to indicate a stable miscibility gap in the calcic amphibole series (the “actinolite–hornblende miscibility gap”), manifesting as either a solvus or a transition loop (e.g., Klein 1969; Cooper and Lovering 1970; Smelik et al. 1991; Begin and Carmichael 1992; Zingg 1996). However, a number of papers have argued that the observation may be better explained by disequilibrium involving preservation of the lower grade amphibole phase (actinolite) as a relic in higher grade hornblende-bearing assemblages (Graham 1974; Grapes 1975; Sampson and Fawcett 1977; Grapes and Graham 1978).

A number of pieces of evidence may support the presence of a miscibility gap including: (1) textural features of stable coexistence including regular sharp intergrowths and, in particular, exsolution microstructures; (2) the presence of a compositional gap between the coexisting amphiboles which shrinks with progressive metamorphism at higher T, representing the closure of a miscibility gap, whether a solvus or transition loop; and (3) the observation of a regular sized compositional gap identifiable in compilations of actinolite and hornblende compositional data from different sequences.

By contrast, the disequilibrium model described in Grapes and Graham (1978) suggests that rather than a gradual increase in the tschermakite content of hornblende with increasing grade, the tschermakite content increases abruptly in a discrete interval that they ascribe to progress of marked reaction within the greenschist–amphibolite facies transition. The result is a compositional gap between actinolite and hornblende, with the actinolite representing a metastable relic from incomplete reaction to hornblende. In this

scenario, coexisting actinolite and hornblende represent disequilibrium pairs, with the hornblende compositions controlled by the degree of overstepping of the hornblende-in reaction. The size of the compositional gap is thus likely to be highly variable, as the nature of the hornblende-forming reactions across the greenschist–amphibolite transition, and the degree to which they may be overstepped, is a function of a number of variables including the  $P$ – $T$  path and bulk rock composition.

### Evidence for an actinolite–hornblende miscibility gap

The data from Flin Flon, Rosslund (Group 1 amphiboles) and most of the sequences described in the literature show a regular compositional gap between actinolite and hornblende in terms of the tschermakite and edenite substitution, which seems incompatible with a primarily kinetically controlled process in which a highly variable pattern of compositional variation might be expected. Rather, such a consistent gap is better explained by the presence of a stable miscibility gap between actinolite and hornblende. A comparison of the amphibole textures and compositions from Flin Flon and Rosslund with those from the literature provides several other lines of evidence for the existence of an actinolite–hornblende miscibility gap. The most convincing textural evidence is the discovery of exsolution microstructures between actinolite and hornblende by Smelik et al. (1991), and the similarity of the compositions of these exsolution lamellae to the actinolite and hornblende compositions from Flin Flon and Rosslund (Fig. 8). Further evidence comes from the documentation of a comparable compositional gap, manifested in terms of a break in the tschermakite and edenite substitutions, between the orthorhombic amphiboles, gedrite, and anthophyllite (Fig. 9). The similarity of the gap between these two sets of amphibole pairs is unlikely to be explained by disequilibrium and overstepping of reactions given that they form from completely different reactions at different  $P$ – $T$ – $X$  conditions. We therefore interpret that an actinolite–hornblende miscibility gap exists and that hornblende initially crystallized at Flin Flon and Rosslund in equilibrium with actinolite across this stable miscibility gap.

### Disequilibrium relationships above the oligoclase-in isograd at Flin Flon

Whilst the textural and compositional data listed above strongly support the presence of an actinolite–hornblende miscibility gap, the evolution of textures and compositions within the Flin Flon sequence seems inconsistent with actinolite and hornblende maintaining equilibrium at higher grade above the oligoclase-in isograd. This is supported by two main observations: (1) an increase in the size of the compositional gap above the oligoclase-in isograd, rather

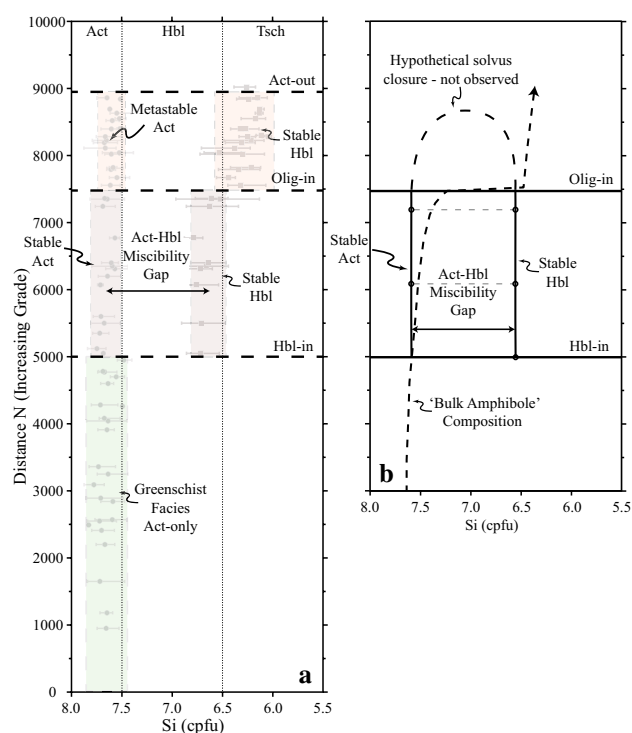


**Fig. 11** Annotated compositional diagram and schematic showing the proposed model for the evolution of the amphibole compositions from the Flin Flon sequence. **a** Annotated compositional diagram showing the evolution of the compositional analyses with increasing grade (distance  $N$ ). **b** Schematic diagram showing interpretation of the compositions with regard to the actinolite–hornblende miscibility gap

than narrowing or closure of the compositional gap; (2) an increasing number of core-rim microstructures within the highest grade samples. Figure 11 illustrates a model that may explain the initial equilibrium coexistence of actinolite and hornblende across a miscibility gap within the hornblende–actinolite zone, followed by divergence in compositions above the oligoclase-in isograd due to disequilibrium processes. Upgrade of the hornblende-in isograd but below the oligoclase-in isograd, the integrated amphibole composition in chemical communication with the other minerals in the rock (here termed the ‘bulk amphibole’ composition, equal to the combined modes and compositions of the stable amphibole phases) falls within the actinolite–hornblende miscibility gap, resulting in stable coexisting actinolite and hornblende. As the oligoclase-in isograd is crossed, there is a marked increase in oligoclase and hornblende at the expense of albite and actinolite, in addition to the hornblende becoming significantly more aluminous in composition. This reflects the ‘bulk amphibole’ composition exiting the aluminous side of the miscibility gap, creating a more aluminous hornblende phase within the hornblende–actinolite–oligoclase zone at Flin Flon. At this point, hornblende

is the only stable amphibole phase within the rock and the equilibrium ‘bulk amphibole’ composition shown in Fig. 11b represents the composition of this more aluminous hornblende. Actinolite and hornblende are no longer interpreted to be in equilibrium across a miscibility gap but actinolite, however, is preserved for a considerable distance up grade as a metastable relic.

Thus, the coexistence of actinolite and hornblende at Flin Flon is interpreted to be a product of equilibrium processes (within the hornblende–actinolite zone) and disequilibrium processes (upgrade of the oligoclase-in isograd within the hornblende–actinolite–oligoclase zone). In this interpretation, only the compositions of actinolite and hornblende below the oligoclase-in isograd are considered to be representative of equilibrium compositions across a stable hornblende–actinolite miscibility gap.

### Rosslund group 2 amphiboles

The Group 2 amphiboles in the Rosslund suite consist of a spread of amphibole compositions, several of which fall within the actinolite–hornblende compositional gap. Similar observations of patchy amphiboles with intermediate compositions were made by Grapes (1975) and Grapes and Graham (1978) that led them to question the existence of a stable miscibility gap. However, the metamorphic replacement of original igneous mineralogy within the Rosslund sequence, in contrast to those at Flin Flon, is patchy with extensive preservation of original igneous pyroxene and amphibole. Metamorphic amphibole commonly only forms as irregular, patchy rims around igneous pyroxene and amphibole grains (e.g., Fig. 2f). The texture of these grains suggests growth of the metamorphic amphiboles may have been triggered by the influx of fluid along grain boundaries, resulting in only minor replacement of the igneous grains and partial equilibration between actinolite, hornblende, and the original igneous amphibole/pyroxene. This rapid growth and partial equilibration between actinolite and hornblende may result in a spread of compositions between the two as observed within the Rosslund Group 2 amphiboles.

### Albite and oligoclase

The coexistence of albite and oligoclase in the Flin Flon and Rosslund sequences is attributed to the widely accepted existence of a miscibility gap (An contents between ~1 and 25%) termed the peristerite gap (e.g., Carpenter 1981; Maruyama et al. 1982). The peristerite gap has been interpreted to represent an asymmetric solvus (e.g., Crawford 1966; Maruyama et al. 1982) though observations indicating that the gap occurs between albite with an ordered low-albite structure and oligoclase with a disordered high-to-intermediate-albite structure has been suggested to be

more consistent with either a two-phase binary loop (e.g., Ashworth and Evirgen 1985b) or a ‘conditional solvus’ (Carpenter 1981). The data from the Flin Flon sequence show that there is no consistent trend in the composition of albite and oligoclase with increasing grade. This may suggest that for the portion of the peristerite gap represented within the Flin Flon sequence, the miscibility gap is characterized by straight limbs with no closure of the gap. However, such an interpretation contrasts with a number of other studies (Maruyama et al. 1982; Grapes and Otsuki 1983; Ashworth and Evirgen 1985a) that have documented an asymmetrical gap characterized by a straight sodic limb and a more shallowly sloping calcic limb. One possibility is that the data from the Flin Flon sequence simply do not capture the top of the peristerite gap as the highest grade samples still contain up to 30–40% albite (Fig. 6b) and thus the shape of the top part of the gap is not observed. An alternative explanation is that, like the coexisting calcic amphiboles, the plagioclase pairs crystallise across a miscibility gap but do not necessarily maintain equilibrium going upgrade and thus the compositions do not represent the shape of the gap in  $P$ – $T$ – $X$  space. In this case, whilst the shape of the miscibility gap may indeed be strongly asymmetric, sluggish kinetics mean that the plagioclase compositions do not maintain equilibrium and instead retain the compositions acquired upon initial crystallization.

Observations and interpretations of the data from the Rosslund sequence are limited by the paucity of coexisting albite–oligoclase pairs. General points that can be made, comparing the data with the Flin Flon sequence, include: (1) there is a greater range of compositions both for albite and oligoclase; (2) albite compositions have slightly higher Ca contents (RV average: An<sub>5.9</sub>; range: An<sub>1–8</sub>, compared to FF average: An<sub>3.2</sub>; range: An<sub>1.1–5.8</sub>); and (3) oligoclase compositions have higher Ca contents (RV range: An<sub>24–34</sub>, compared to FF average: An<sub>22.3</sub>; range: An<sub>17.5–26.0</sub>).

Oligoclase compositions coexisting with albite within the Rosslund sequence show a large range of compositions (~An<sub>24–34</sub>), unusual for a mineral coexisting across a miscibility gap. Similar observations as observed at Rosslund were made by Maruyama et al. (1982), who documented a gap in compositions between albite and oligoclase (An<sub>5</sub>–An<sub>17</sub>) but found that the oligoclase grains displayed a range of compositions (An<sub>17</sub>–An<sub>29</sub>).

Figure 12 shows a  $T$ – $X_{\text{An}}$  diagram, modified from Maruyama et al. (1982), showing an interpretation of the evolution of plagioclase compositions across the greenschist–amphibolite transition zone. Between  $T_1$  and  $T_2$ , both albite and oligoclase are stable with compositions corresponding to the limbs of the peristerite gap. With increasing temperature, the integrated plagioclase composition in chemical communication with the other minerals in the rock (here termed the ‘bulk plagioclase’ composition) shifts to higher Ca contents

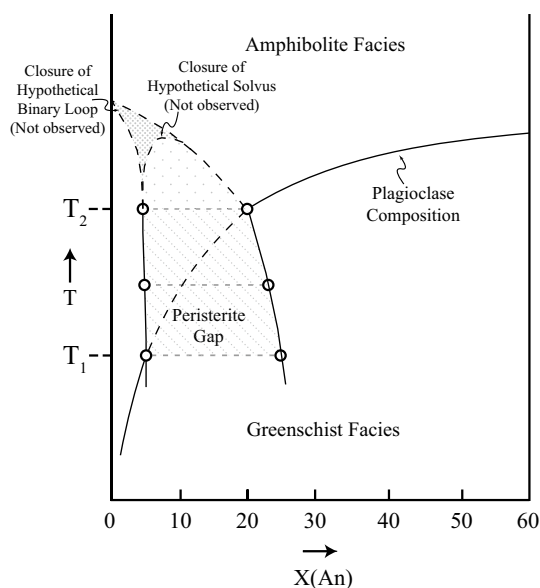


**Fig. 12** Schematic diagram showing evolving plagioclase compositions across the greenschist–amphibolite transition zone and the relationship to the peristerite gap. Modified from Maruyama et al. (1982)

before exiting the miscibility gap at  $T_2$  (Fig. 12). As a result, the closure of the peristerite gap, which may take the form of a solvus or binary loop (Fig. 12), is not observed. Above  $T_2$ , the plagioclase compositions become progressively more calcic. Thus, the range of plagioclase compositions at Rosslund may be explained by a two-stage model: (1) initial crystallisation across the peristerite gap (between  $T_1$  and  $T_2$ ); and (2) movement out of the peristerite gap (above  $T_2$ ), resulting in more Ca-rich oligoclase coexisting with relic albite that persists metastably upgrade.

### Epidote group minerals

Previous studies have attributed the observed gaps in the clinozoisite–epidote series to either miscibility gaps (e.g., Strens 1963, 1964; Grapes and Hoskin 2004) or the metastable persistence of an earlier generation of epidote due to sluggish reaction kinetics (Bird and Helgeson 1981). Strens (1965) argued that there are crystal–chemical reasons for anticipating the existence of a miscibility gap between Fe-rich and Fe-poor epidote, resulting from increased structural strain within an epidote when the large Fe and small Al ions occupy adjacent octahedral sites.

The high density of samples at Flin Flon provides a good dataset with which to test the possible existence of a miscibility gap. Figure 6c demonstrates that there is a chemical discontinuity between core and rim compositions in most samples, though the size and position of the compositional gaps are variable. Epidote cores are characterized by  $X_{Ps}$  contents ranging between 18–32% compared to

$X_{Ps} = 13–25\%$  for more Al-rich rims. Thus whilst a compositional gap exists in most individual samples, there is overlap between core and rim compositions across different samples with no well-defined overall compositional gap. In addition, there is commonly a large range in compositions within samples and single grains. In samples that contain patchy irregular zoning (Fig. 7d), different patches display variable compositions and diffuse contacts.

A comparison of the data from the literature and this study shows that the size and positioning of the compositional gap amongst different sequences are also highly variable (Fig. 10). The data from these natural datasets also show differences from the experimental solvi of Fehr and Heuss-Abbichler (1997), with the natural epidotes mostly containing compositional gaps larger than those observed in the experiments. Thus, whilst solvi may exist at the conditions used in the experimental studies (5 kbar; > 500 °C; Fehr and Heuss-Abbichler 1997), they do not appear to be represented in the data from greenschist–amphibolite sequences. Instead, we interpret the common development of an iron-poor rim surrounding an iron-rich core to be due to sequential growth of two generations of epidote.

Observations from Flin Flon and Rosslund suggest that the zoned epidote grains first appear in the lower greenschist facies and are not present within the prehnite–pumpellyite facies, similar to observations from other studies of prehnite–pumpellyite and greenschist facies sequences (Grapes and Hoskin 2004 and reference therein). This suggests that the growth of the more Fe-poor epidote rims may result from reactions occurring across the prehnite–pumpellyite-to-greenschist transition. Rather than equilibration with the lower grade Fe-rich epidote cores, the Fe-poor epidote forms rims that are then maintained going upgrade into the greenschist and lower amphibolite facies. Comparison of textures, modal abundances, and compositions of epidote (Fig. 6c, d) suggests that epidote remains as an inert phase during prograde metamorphism and is not significantly involved in the hornblende and oligoclase-forming reactions at the greenschist–amphibolite transition. If so, epidote crystals with core and rim microstructures that formed at lower  $P$ – $T$  conditions may have been preserved.

### Controls on devolatilization reactions across the greenschist–amphibolite transition zone

The release of fluids due to metamorphic devolatilization occurring across the greenschist–amphibolite facies transition carries important implications for geochemical cycling within greenstone belts, as well as for the formation of economically valuable ore deposits such as orogenic gold deposits (e.g., Powell et al. 1991; Elmer et al. 2006; Phillips and Powell 2010). A number of studies have assessed the nature of these devolatilization reactions using

an equilibrium thermodynamic modelling approach (e.g., Powell et al. 1991; Elmer et al. 2006), and have detailed the equilibrium evolution of fluid-producing reactions (Elmer et al. 2006). However, studies of natural sequences have been hampered by the fine-grained and heterogeneous nature of rocks at this metamorphic grade. Our high-resolution study of the exceptionally well exposed greenschist–amphibolite transition at Flin Flon, augmented with data from Rosslund, provides constraints from field and petrographic observations on the relative importance of different devolatilization reactions, the modal changes in the key hydrous minerals, and the degree to which the dehydration occurs over a wide or narrow spatial (and hence thermal) interval.

Previous studies of the greenschist–amphibolite transition zone have identified a number of reactions that may play a role in the transition from a greenschist-to-amphibolite facies assemblage (e.g., Cooper 1972; Graham 1974; Laird 1982; Maruyama et al. 1983; Begin 1992). For moderate-pressure (Barrovian) prograde sequences (> 5 kbar; Begin 1992), such as at Flin Flon, the mineralogical transformation is anticipated to occur first through the formation of hornblende through the breakdown of actinolite, epidote, albite, and chlorite [reaction (1) and (2)] above the hornblende-in isograd (e.g., Cooper 1972; Graham 1974; Begin 1992). At higher temperatures, upon crossing the oligoclase-in isograd, further breakdown of chlorite and epidote occurs concomitant with the formation of oligoclase and hornblende (reaction (3)) (e.g., Cooper 1972; Graham 1974; Begin 1992).

In contrast to this progressive series of devolatilization reactions, observations from the Flin Flon sequence suggest the majority of the mineralogical transformation happens over a thin zone (~ 1500 m thickness), proceeding only at higher grades after the appearance of oligoclase upgrade of the oligoclase-in isograd (Figs. 4, 6). Within the greenschist facies and lower part of the greenschist–amphibolite transition (below the oligoclase-in isograd), there is little apparent reaction progress, with only minor hornblende production and minimal hydrous-phase breakdown (Figs. 4, 6). By contrast, significant change in the mineral assemblage and modal proportions occurs across the oligoclase-in isograd, with large increases in hornblende and oligoclase, at the expense of actinolite, albite, and chlorite (Figs. 4, 6). Actinolite, however, remains as a metastable relic a considerable distance upgrade of the oligoclase-in isograd.

The most significant modal change across this interval in terms of the metamorphic devolatilization is the marked reduction in the amount of chlorite, which contains the majority of the mineral-bound water in the rock. By contrast, epidote, one of the other major hydrous phases in the rock shows no decrease in modal proportions (Fig. 6c, d) and is not a major contributor to fluid production across the transition. Modal estimates suggest the loss of approximately 11% chlorite across the hornblende–actinolite–oligoclase

zone (from a modal average of 15% in the greenschist facies and hornblende–actinolite zone to an average of 4% at the top of the hornblende–actinolite–oligoclase zone), resulting in devolatilization of approximately 1.1–1.8 wt% H<sub>2</sub>O (depending on bulk composition). The textural, modal, and compositional observations from the Flin Flon sequence suggest that the incoming of oligoclase is key to initiating this devolatilization across the greenschist–amphibolite transition zone. Upon crossing the oligoclase-in isograd, significant reaction progress occurs across a narrow zone within the field (1500 m). The result is a substantial pulse of rock devolatilization over a small spatial and thermal interval.

### Implications for deriving miscibility gap limits from natural data sets

Given the lack of experimental data on the  $P$ – $T$ – $X$  limits of miscibility gaps within many of the common mineral series, datasets from natural sequences have played a crucial role, particularly for amphibole (e.g., Grapes and Graham 1978; Robinson 1982; Zingg 1996; Schumacher 2007), epidote (e.g., Enami et al. 2004; Grapes and Hoskin 2004), and plagioclase (e.g., Maruyama et al. 1982; Grapes and Otsuki 1983). Natural datasets form the basis for the current calibration of thermodynamic  $a$ – $X$  models for amphibole (Dale et al. 2005; Diener et al. 2007; Diener and Powell 2012).

The extensive textural, modal, and compositional data across the transition from prehnite–pumpellyite facies to lower amphibolite facies from the Flin Flon and Rosslund sequences provide a unique high-resolution dataset for studying the equilibrium and disequilibrium relationships between coexisting minerals. Whereas the data provide strong evidence for the existence of equilibrium miscibility gaps within the actinolite–hornblende and albite–oligoclase series, they also provide evidence for disequilibrium relationships. Distinguishing between the two is essential if natural datasets are to be used to identify and characterise miscibility gaps, and more broadly to extract thermodynamic data and  $a$ – $X$  relations.

The data from this study show that whilst two minerals may crystallize in equilibrium across a miscibility gap, the thermodynamic driving force to maintain equilibrium across this miscibility gap going up grade may not be enough to overcome the sluggish kinetics at these low-to-moderate  $P$ – $T$  conditions. At Flin Flon and Rosslund, the variation in composition of amphibole, plagioclase and epidote, upgrade of the first appearance of hornblende and oligoclase, do not reflect the compositional limits of miscibility gaps, instead reflecting disequilibrium relationships. In addition, the modal, textural, and compositional features of epidote indicate that it did not participate in the hornblende- and oligoclase-forming reactions, instead appearing to remain

unreactive. Prograde unreactivity of epidote minerals was also described by Pattison and Seitz (2012).

Most sequences containing coexisting actinolite and hornblende show little evidence for the convergence of compositions with increasing grade (e.g., Robinson 1982; Schumacher 2007). Schumacher (2007) found that a compilation of actinolite–hornblende data showed that a gap existed but did not define the shape of a solvus. Our interpretation of the Flin Flon sequence suggests that whilst the coexisting amphiboles initially crystallized across a miscibility gap, the compositions going upgrade do not trace the shape of a miscibility gap. Instead the equilibrated hornblende becomes increasingly aluminous while actinolite persists upgrade as a metastable relic. A similar relationship between albite and oligoclase is the best explanation for the observations from the Rosslund sequence and the data of Maruyama et al. (1982). Ignoring the disequilibrium aspects of the evolution of coexisting amphiboles and plagioclase group minerals in the Flin Flon and Rosslund sequences would lead to erroneous interpretation of the size and shape of the miscibility gaps in  $P$ – $T$ – $X$  space, and therefore of amphibole  $a$ – $X$  models. It is suggested that the detailed documentation of coexisting mineral data with respect to changing grade, such as carried out in this study, is essential for the accurate identification of equilibrium and disequilibrium relationships and the characterization of miscibility gaps from natural datasets.

## Conclusions

1. The textural and compositional data from Flin Flon and Rosslund, combined with a compilation of data from the literature, support the existence of stable miscibility gaps within the actinolite–hornblende and albite–oligoclase series.
2. However, the evolution of the compositions and textures of actinolite and hornblende, and of albite and oligoclase, upgrade of the first (prograde) appearance of hornblende and oligoclase are not consistent with the pairs of minerals maintaining equilibrium once crystallized. Actinolite and hornblende compositions diverge upgrade of the oligoclase-in isograd, interpreted to be due to growth of an increasingly aluminous hornblende from chlorite breakdown, and metastable persistence of actinolite relics.
3. Compositional gaps and core-rim microstructures within the epidote series are best explained as progressive mineral overgrowths and preservation of a lower grade epidote phase to higher  $P$ – $T$  conditions. Assessment of textural and compositional data from Flin Flon and the literature suggests that the common observation of mul-

tipple epidote group phases does not indicate the presence of a miscibility gap at these  $P$ – $T$  conditions.

4. A focused pulse of metamorphic devolatilization occurs within the greenschist–amphibolite facies transition. At Flin Flon, it occurs over a narrow spatial and thermal interval immediately upgrade of the oligoclase-in isograd, primarily resulting from the breakdown of chlorite.
5. The observations from this paper emphasize the difficulty in distinguishing equilibrium and disequilibrium features of coexisting minerals in metamorphic sequences. Using compilations of natural mineral compositional data to construct the  $P$ – $T$ – $X$  and  $a$ – $X$  relationships of miscibility gaps is problematic due to the difficulty in interpreting which compositions reflect the equilibrium compositional limits of the gap. Assuming the data represent equilibrium relationships will result in erroneous predictions if the natural data reflect, wholly or in part, disequilibrium processes. Detailed documentation of textures and compositions with changing grade in well characterized sequences, such as Flin Flon, are essential to distinguishing the two.

**Acknowledgements** We acknowledge R. Marr for help with operating the electron microprobe at the University of Calgary. E.D. Ghent is thanked for advice regarding the Rosslund field area. We are grateful to D.E. Ames, S.G. Digel, W.G. Powell and E.D. Ghent for providing us with access to samples from Flin Flon and Rosslund. We thank Frank Spear, an anonymous reviewer and the editor Daniela Rubatto for their constructive and insightful reviews that helped improve this manuscript. This research was supported by NSERC Discovery Grant 037233 to Pattison.

## References

- Allen J, Goldie R (1978) Coexisting amphiboles from the Noranda area, Quebec; extension of the actinolite–hornblende miscibility gap to iron-rich bulk compositions. *Am Mineral* 63:205–209
- Ames D, Galley A, Kjarsgaard I, Tardif N, Taylor B (2016) Hanging-wall vectoring for buried volcanogenic massive sulfide deposits, Paleoproterozoic Flin Flon mining camp, Manitoba, Canada. *Econ Geol* 111:963–1000
- Ansdell KM (2005) Tectonic evolution of the Manitoba–Saskatchewan segment of the Paleoproterozoic Trans-Hudson Orogen, Canada. *Can J Earth Sci* 42:741–759
- Ashworth J, Evirgen M (1985a) Plagioclase relations in pelites, central Menderes Massif, Turkey. I. The peristerite gap with coexisting kyanite. *J Metamorph Geol* 3:207–218
- Ashworth J, Evirgen M (1985b) Plagioclase relations in pelites, central Menderes Massif, Turkey. II. Perturbation of garnet-plagioclase geobarometers. *J Metamorph Geol* 3:219–229
- Beddoe-Stephens B (1981) Metamorphism of the Rosslund volcanic rocks, southern British Columbia. *Can Mineral* 19:631–641
- Beddoe-Stephens B (1982) The petrology of the Rosslund volcanic rocks, southern British Columbia. *Geol Soc Am Bull* 93:585–594
- Begin N (1992) Contrasting mineral isograd sequences in metabasites of the Cape Smith Belt, northern Quebec, Canada: three new bathograds for mafic rocks. *J Metamorph Geol* 10:685–704

- Begin NJ, Carmichael DM (1992) Textural and compositional relationships of Ca-amphiboles in metabasites of the Cape Smith Belt, northern Québec: implications for a miscibility gap at medium pressure. *J Petrol* 33:1317–1343
- Bird DK, Helgeson HC (1981) Chemical interaction of aqueous solutions with epidote–feldspar mineral assemblages in geologic systems. II. Equilibrium constraints in metamorphic/geothermal processes. *Am J Sci* 281:576–614
- Bishop D (1972) Progressive metamorphism from prehnite–pumpellyite to greenschist facies in the Dansey Pass area, Otago, New Zealand. *Geol Soc Am Bull* 83:3177–3198
- Boyle AP (1986) Metamorphism of basic and pelitic rocks at Sulitjelma, Norway. *Lithos* 19:113–128
- Brady JB (1974) Coexisting actinolite and hornblende from west-central New Hampshire. *Am Mineral* 59:529–535
- Bucher-Nurminen K (1982) Mechanism of mineral reactions inferred from textures of impure dolomitic marbles from East Greenland. *J Petrol* 23:325–343
- Carpenter MA (1981) A “conditional spinodal” within the peristerite miscibility gap of plagioclase feldspars. *Am Mineral* 66:553–560
- Champness P, Rodgers K (2000) The origin of iridescence in anthophyllite–gedrite from Simiuttat, Nuuk district, southern West Greenland. *Mineral Mag* 64:885–889
- Choudhuri A (1974) Distribution of Fe and Mg in actinolite, hornblende and biotite in some precambrian metagreywackes from Guyana, South America. *Contrib Mineral Petrol* 44:45–55
- Compton RR (1958) Significance of amphibole paragenesis in the Bidwell Bar region, California. *Am Mineral* 43:890–907
- Cooper A (1972) Progressive metamorphism of metabasic rocks from the Haast Schist Group of southern New Zealand. *J Petrol* 13:457–492
- Cooper A, Lovering J (1970) Greenschist amphiboles from Haast River, New Zealand. *Contrib Mineral Petrol* 27:11–24
- Crawford ML (1966) Composition of plagioclase and associated minerals in some schists from Vermont, USA, and South Westland, New Zealand, with inferences about the peristerite solvus. *Contrib Mineral Petrol* 13:269–294
- Dale J, Powell R, White R, Elmer F, Holland T (2005) A thermodynamic model for Ca–Na clin amphiboles in  $\text{Na}_2\text{O}$ – $\text{CaO}$ – $\text{FeO}$ – $\text{MgO}$ – $\text{Al}_2\text{O}_3$ – $\text{SiO}_2$ – $\text{H}_2\text{O}$ – $\text{O}$  for petrological calculations. *J Metamorph Geol* 23:771–791
- DeWolfe Y, Gibson H (2006) Stratigraphic subdivision of the Hidden and Louis formations, Flin Flon, Manitoba (NTS 63K16SW). Report of activities 2006, Manitoba science, technology, energy and mines, Manitoba geological survey, pp 22–34
- DeWolfe Y, Gibson H, Lafrance B, Bailes A (2009) Volcanic reconstruction of Paleoproterozoic arc volcanoes: the Hidden and Louis formations, Flin Flon, Manitoba, Canada. *Can J Earth Sci* 46:481–508
- Diener J, Powell R (2012) Revised activity–composition models for clinopyroxene and amphibole. *J Metamorph Geol* 30:131–142
- Diener J, Powell R, White R, Holland T (2007) A new thermodynamic model for clino- and orthoamphiboles in the system  $\text{Na}_2\text{O}$ – $\text{CaO}$ – $\text{FeO}$ – $\text{MgO}$ – $\text{Al}_2\text{O}_3$ – $\text{SiO}_2$ – $\text{H}_2\text{O}$ – $\text{O}$ . *J Metamorph Geol* 25:631–656
- Digel SG, Gordon TM (1995) Phase relations in metabasites and pressure–temperature conditions at the prehnite–pumpellyite to greenschist facies transition, Flin Flon, Manitoba, Canada. *Geol Soc Am Spec Pap* 296:67–80
- Droop G (1987) A general equation for estimating  $\text{Fe}^{3+}$  concentrations in ferromagnesian silicates and oxides from microprobe analyses, using stoichiometric criteria. *Mineral Mag* 51:431–435
- Elmer F, White R, Powell R (2006) Devolatilization of metabasic rocks during greenschist–amphibolite facies metamorphism. *J Metamorph Geol* 24:497–513
- Enami M, Liou J, Mattinson C (2004) Epidote minerals in high P/T metamorphic terranes: subduction zone and high- to ultrahigh-pressure metamorphism. *Rev Mineral Geochem* 56:347–398
- Fehr KT, Heuss-Aßbichler S (1997) Intracrystalline equilibria and im-miscibility along the join clinozoisite–epidote: an experimental and  $^{57}\text{Fe}$  Mössbauer study. *Neues Jahrbuch für Mineralogie-Abhandlungen* 172:43–67
- Franz G, Liebscher A (2004) Physical and chemical properties of the epidote minerals—an introduction. *Rev Mineral Geochem* 56:1–81
- Franz G, Selverstone J (1992) An empirical phase diagram for the clinozoisite–zoisite transformation in the system  $\text{Ca}_2\text{Al}_3\text{Si}_3\text{O}_{12}(\text{OH})$ – $\text{Ca}_2\text{Al}_2\text{Fe}^{3+}\text{Si}_3\text{O}_{12}(\text{OH})$ . *Am Mineral* 77:631–642
- Frimmel H (1996) Witwatersrand iron-formations and their significance for gold genesis and the composition limits of orthoamphibole. *Mineral Petrol* 56:273–295
- Gale D, Lucas S, Dixon J (1999) Structural relations between the poly-deformed Flin Flon arc assemblage and Missi Group sedimentary rocks, Flin Flon area, Manitoba and Saskatchewan. *Can J Earth Sci* 36:1901–1915
- Ghosh DK (1995) U–Pb geochronology of Jurassic to early Tertiary granitic intrusives from the Nelson–Castlegar area, southeastern British Columbia, Canada. *Can J Earth Sci* 32:1668–1680
- Graham CM (1974) Metabasite amphiboles of the Scottish Dalradian. *Contrib Mineral Petrol* 47:165–185
- Grapes RH (1975) Actinolite–hornblende pairs in metamorphosed gabbros, Hidaka Mountains, Hokkaido. *Contrib Mineral Petrol* 49:125–140
- Grapes RH, Graham CM (1978) The actinolite–hornblende series in metabasites and the so-called miscibility gap: a review. *Lithos* 11:85–92
- Grapes RH, Hoskin P (2004) Epidote group minerals in low–medium pressure metamorphic terranes. *Rev Mineral Geochem* 56:301–345
- Grapes RH, Otsuki M (1983) Peristerite compositions in quartzofeldspathic schists, Franz Josef–Fox Glacier area, New Zealand. *J Metamorph Geol* 1:47–61
- Hawthorne FC, Oberti R (2007) Classification of the amphiboles. *Rev Mineral Geochem* 67:55–88
- Hawthorne FC, Oberti R, Harlow GE, Maresch WV, Martin RF, Schumacher JC, Welch MD (2012) Nomenclature of the amphibole supergroup. *Am Mineral* 97:2031–2048
- Heuss-Aßbichler S, Fehr KT (1997) Intercrystalline exchange of Al and  $\text{Fe}^{3+}$  between grossular–andradite and clinozoisite–epidote solid solutions. *Neues Jahrbuch für Mineralogie-Abhandlungen* 172:69–100
- Hietanen A (1974) Amphibole pairs, epidote minerals, chlorite, and plagioclase in metamorphic rocks, Northern Sierra Nevada, California. *Am Mineral* 59:2240
- Hoffman PF (1988) United plates of America, the birth of a craton: Early Proterozoic assembly and growth of Laurentia. *Annu Rev Earth Planet Sci* 16:543–603
- Holdaway MJ (1965) Basic regional metamorphic rocks in part of the Klamath Mountains, Northern California. *Am Mineral* 50:953–977
- Holland T, Blundy J (1994) Non-ideal interactions in calcic amphiboles and their bearing on amphibole–plagioclase thermometry. *Contrib Mineral Petrol* 116:433–447
- Höy T, Dunne KP (2001) Metallogeny and mineral deposits of the Nelson–Rossland map-area. Part II, The Early Jurassic Rossland group, southeastern British Columbia. *B C Minist Energy Mines Bull* 109:1–195
- Janák M, Hurai V, Ludhová L, Thomas R (1999) Partial melting and retrogression during exhumation of high-grade metapelites, the Tatra Mountains, Western Carpathians. *Phys Chem Earth* 24:289–294

- Katagas C, Panagos A (1979) Pumpellyite–actinolite and greenschist facies metamorphism in Lesvos island (Greece). *Mineral Petrol* 26:235–254
- Klein C Jr (1969) Two-amphibole assemblages in the system actinolite–hornblende–glaucophane. *Am Mineral* 54:212–237
- Lafrance B, Gibson HL, Pehrsson S, Schetselaar E, DeWolfe YM, Lewis D (2016) Structural reconstruction of the Flin Flon volcanogenic massive sulfide mining district, Saskatchewan and Manitoba, Canada. *Econ Geol* 111:849–875
- Laird J (1982) Phase relations of metamorphic amphiboles; natural occurrence and theory; amphiboles in metamorphosed basaltic rocks; greenschist facies to amphibolite facies. *Rev Mineral Geochem* 9:113–138
- Leake BE, Woolley AR, Arps CE, Birch WD, Gilbert MC, Grice JD, Hawthorne FC, Kato A, Kisch HJ, Krivovichev VG (1997) Report. Nomenclature of amphiboles: report of the subcommittee on amphiboles of the international mineralogical association commission on new minerals and mineral names. *Mineral Mag* 61:295–321
- Lucas S, Stern R, Syme E, Reilly B, Thomas D (1996) Intraoceanic tectonics and the development of continental crust: 1.92–1.84 Ga evolution of the Flin Flon Belt, Canada. *Geol Soc Am Bull* 108:602–629
- Maruyama S, Liou J, Suzuki K (1982) The peristerite gap in low-grade metamorphic rocks. *Contrib Mineral Petrol* 81:268–276
- Maruyama S, Suzuki K, Liou J (1983) Greenschist–amphibolite transition equilibria at low pressures. *J Petrol* 24:583–604
- Misch P, Rice J (1975) Miscibility of tremolite and hornblende in progressive Skagit metamorphic suite, North Cascades, Washington. *J Petrol* 16:1–21
- Morteani G, Raase P (1974) Metamorphic plagioclase crystallization and zones of equal anorthite content in epidote-bearing, amphibole-free rocks of the western Tauernfenster, eastern Alps. *Lithos* 7:101–111
- Pattison DRM, Seitz JL (2012) Stabilization of garnet in metamorphosed altered turbidites near the St. Eugene lead–zinc deposit, southeastern British Columbia: equilibrium and kinetic controls. *Lithos* 134:221–235
- Pattison DRM, Tinkham D (2009) Interplay between equilibrium and kinetics in prograde metamorphism of pelites: an example from the Nelson aureole, British Columbia. *J Metamorph Geol* 27:249–279
- Pattison DRM, Vogl JJ (2005) Contrasting sequences of metapelitic mineral-assemblages in the aureole of the Tilted Nelson Batholith, British Columbia: implications for phase equilibria and pressure determination in andalusite–sillimanite-type settings. *Can Mineral* 43:51–88
- Phillips G, Powell R (2010) Formation of gold deposits: a metamorphic devolatilization model. *J Metamorph Geol* 28:689–718
- Powell WG, Ghent ED (1996) Low-pressure metamorphism of the mafic volcanic rocks of the Rossland Group, southeastern British Columbia. *Can J Earth Sci* 33:1402–1409
- Powell R, Will T, Phillips G (1991) Metamorphism in Archaean greenstone belts: calculated fluid compositions and implications for gold mineralization. *J Metamorph Geol* 9:141–150
- Raith M (1976) The Al–Fe(III) epidote miscibility gap in a metamorphic profile through the Penninic Series of the Tauern Window, Austria. *Contrib Mineral Petrol* 57:99–117
- Robinson P (1982) Phase relations of metamorphic amphiboles: Natural occurrences and theory. *Rev Mineral Geochem* 9:1–227
- Robinson P, Jaffe HW (1969) Aluminous enclaves in gedrite-cordierite gneiss from southwestern New Hampshire. *Am J Sci* 267:389–421
- Sampson G, Fawcett J (1977) Coexisting amphiboles from the Hastings region of southeastern Ontario. *Can Mineral* 15:283–296
- Schneiderman JS, Tracy RJ (1991) Petrology of orthoamphibole–cordierite gneisses from the Orijarvi area, Southwest Finland. *Am Mineral* 76:942–955
- Schreyer W, Abraham K (1978) Symplectitic cordierite–orthopyroxene–garnet assemblages as products of contact metamorphism of pre-existing basement granulites in the Vredefort structure, South Africa, and their relations to pseudotachylite. *Contrib Mineral Petrol* 68:53–62
- Schumacher JC (1997) Appendix 2: the estimation of the proportion of ferric iron in the electron-microprobe analysis of amphiboles. *Can Mineral* 35:238–246
- Schumacher JC (2007) Metamorphic amphiboles: composition and coexistence. *Rev Mineral Geochem* 67:359–416
- Sevigny J, Parrish R (1993) Age and origin of late Jurassic and Paleocene granitoids, Nelson Batholith, southern British Columbia. *Can J Earth Sci* 30:2305–2314
- Smelik EA, Veblen DR (1993) A transmission and analytical electron microscope study of exsolution microstructures and mechanisms in the orthoamphiboles anthophyllite and gedrite. *Am Mineral* 78:511–532
- Smelik EA, Nyman MW, Veblen DR (1991) Pervasive exsolution within the calcic amphibole series; TEM evidence for a miscibility gap between actinolite and hornblende in natural samples. *Am Mineral* 76:1184–1204
- Spear FS (1980) The gedrite–anthophyllite solvus and the composition limits of orthoamphibole from the Post Pond Volcanics, Vermont. *Am Mineral* 65:1103–1118
- Stauffer MR (1984) Manikewan: an early Proterozoic ocean in central Canada, its igneous history and orogenic closure. *Precambrian Res* 25:257–281
- Stern RA, Syme EC, Bailes AH, Lucas SB (1995) Paleoproterozoic (1.90–1.86 Ga) arc volcanism in the Flin Flon Belt, Trans-Hudson Orogen, Canada. *Contrib Mineral Petrol* 119:117–141
- Stout JH (1972) Phase petrology and mineral chemistry of coexisting amphiboles from Telemark, Norway. *J Petrol* 13:99–145
- Strens R (1963) Some relationships between members of the epidote group. *Nature* 198:80–81
- Strens R (1964) Epidotes of the Borrowdale volcanic rocks of central Borrowdale. *Mineral Mag* 33:868–886
- Strens R (1965) Stability and relations of the Al–Fe epidotes. *Mineral Mag* 35:464–475
- Syme E, Bailes A (1993) Stratigraphic and tectonic setting of early Proterozoic volcanogenic massive sulfide deposits, Flin Flon, Manitoba. *Econ Geol* 88:566–589
- Tagiri M (1977) Fe–Mg partition and miscibility gap between coexisting calcic amphiboles from the southern Abukuma Plateau, Japan. *Contrib Mineral Petrol* 62:271–281
- Terabayashi M (1993) Compositional evolution in Ca-amphibole in the Karmutsen metabasites, Vancouver Island, British Columbia, Canada. *J Metamorph Geol* 11:677–690
- Tomkins H, Pattison DRM (2007) Accessory phase petrogenesis in relation to major phase assemblages in pelites from the Nelson contact aureole, southern British Columbia. *J Metamorph Geol* 25:401–421
- Yamaguchi Y (1985) Hornblende–cummingtonite and hornblende–actinolite intergrowths from the Koyama calc-alkaline intrusion, Susa, southwest Japan. *Am Mineral* 70:980–986
- Zingg A (1996) Immiscibility in Ca-amphiboles. *J Petrol* 37:471–496

**Publisher's Note** Springer Nature remains neutral with regard to jurisdictional claims in published maps and institutional affiliations.